



저작자표시-비영리-변경금지 2.0 대한민국

이용자는 아래의 조건을 따르는 경우에 한하여 자유롭게

- 이 저작물을 복제, 배포, 전송, 전시, 공연 및 방송할 수 있습니다.

다음과 같은 조건을 따라야 합니다:



저작자표시. 귀하는 원저작자를 표시하여야 합니다.



비영리. 귀하는 이 저작물을 영리 목적으로 이용할 수 없습니다.



변경금지. 귀하는 이 저작물을 개작, 변형 또는 가공할 수 없습니다.

- 귀하는, 이 저작물의 재이용이나 배포의 경우, 이 저작물에 적용된 이용허락조건을 명확하게 나타내어야 합니다.
- 저작권자로부터 별도의 허가를 받으면 이러한 조건들은 적용되지 않습니다.

저작권법에 따른 이용자의 권리는 위의 내용에 의하여 영향을 받지 않습니다.

이것은 [이용허락규약\(Legal Code\)](#)을 이해하기 쉽게 요약한 것입니다.

[Disclaimer](#)

Master's Thesis of Natural Science

**Application of search-based
Simulation-Optimization model to
suggest optimal pump-and-treat
strategies at DNAPL contaminated site**

탐색 기반 모의-최적화 모델을 활용한 유류 오염
지역 내 최적의 양수-처리 전략 제안

August 2023

Graduate School of Seoul National University
College of Natural Sciences
School of Earth and Environmental Sciences

Suh-Ho Lee

**Application of search-based
Simulation-Optimization model to
suggest optimal pump-and-treat
strategies at DNAPL contaminated site**

Submitting a master's thesis of Natural Science

August 2023

**Graduate School of Seoul National University
College of Natural Science
School of Earth and Environmental Science**

Suh-Ho Lee

Confirming the master's thesis written by

Suh-Ho Lee

August 2023

Chair _____(Seal)

Vice Chair _____(Seal)

Examiner _____(Seal)

Abstract

Groundwater remediation has become a significant challenge in maintaining the value of water resources. Pump-and-treat among the various remediation methods is widely has been used as a remediation technology for trichloroethylene (TCE) contamination in groundwater, but a cost-effective remediation design needs to be formulated. The Genetic Algorithm (GA) which is one of the optimization methods is commonly has been applied to suggest groundwater remediation strategies. However, it has limitations in solving multi-objective optimization problems. As an alternative to this problem, the Non-Dominated Sorting Genetic Algorithm-II (NSGA-II) is being suggested and utilized. This study aims to evaluate the relative performance of NSGA-II in groundwater remediation for solving multi-objective optimization problems and proposes an optimal groundwater remediation design for the highly contaminated alluvial aquifer at the Wonju Industrial Complex (WIC). MODFLOW and MT3D are used to simulate groundwater flow and solute transport in both the benchmark model and the alluvial aquifer model. Additionally, a geostatistical model is applied to generate a heterogeneous hydraulic conductivity field and the concentration distribution of TCE. To assess the performance of NSGA-II, both GA with weighting and NSGA-II are applied to solve the multi-objective optimization problem in the benchmark model. Furthermore, optimal pump-and-treat strategies at WIC are suggested by introducing the Well Contribution Index (WCI), which considers the pumping rate and well specification data such as length of well screen or depth of well. The performance assessment results demonstrate that NSGA-II performs well in solving multi-objective optimization problems for groundwater remediation with conflicting objectives. The results obtained from the alluvial aquifer model indicate that extracting groundwater only during the rainy season can effectively execute the pump-and-treat strategy. Finally, the proposed WCI results indicate that

well KDPW-7 significantly contributes to the pump-and-treat process. Previous pilot tests conducted at KDPW-7 have proved effective remediation, and the findings of this study suggest that the WCI can provide valuable insights for remediation operation strategies such as the selection of pumping wells in real pump-and-treat scenarios.

Keyword: Groundwater modeling, Pump-and-treat, Non-dominated Sorting Genetic Algorithm (NSGA-II), Trichloroethylene (TCE), Well Contribution Index (WCI)

Student Number: 2021-24628

TABLE OF CONTENTS

1	INTRODUCTION	1
1.1	Research Background.....	1
1.2	Objectives and Scope.....	4
2	METHODOLOGY	5
2.1	Site description.....	5
2.2	Numerical model.....	9
2.3	Geostatistical model.....	1 9
2.4	Optimization for pump-and-treat	2 5
2.5	Relative performance assessment.....	2 9
2.6	Factors of optimal pump-and-treat.....	3 1
3	RESULTS AND DISCUSSION.....	3 6
3.1	Benchmark problem	3 6
3.2	Regional scale model.....	4 7
4	CONCLUSION	6 4
5	REFERENCE.....	6 6

LIST OF FIGURES

- Figure 2-1. Site properties which are about (a) location and the source zone of the study area where is Woosan Industrial Complex (WIC) (b) Geological map of the study area. Red box indicates hot source zone and black dots indicate observation wells in this area. Qa and Jbgr indicate Quaternary alluvial deposits and biotite granite, respectively..... 7**
- Figure 2-2. Monthly rainfall data and changes in TCE concentration at observation wells at Woosan Industrial Complex (WIC) site. .. 8**
- Figure 2-3. Model domain and boundary conditions for benchmark problem. Blue cross dots indicate the location of pumping wells. Black rectangular box is TCE source zone. 1 1**
- Figure 2-4. Model grid and boundary conditions for Wonju Industrial Complex (WIC); (a) Model grid design for horizontal direction. (b) Model grid design for vertical direction. Black dots in (a) indicate observation wells. Yellow and red color in (b) indicate alluvial and bedrock layer, respectively..... 1 3**
- Figure 2-5. Boundary conditions assigned for groundwater flow model in WIC. 1 4**
- Figure 2-6. Chemical reaction procedure of PCE and TCE. 1 8**
- Figure 2-7. (a) Crossover and (b) Mutation operators 2 7**

Figure 2-8. Flowchart of Simulation coupled with optimization modeling that uses NSGA-II for optimization..... 2 8

Figure 2-9. Flowchart of relative performance assessment for NSGA-II..... 3 0

Figure 2-10. The location of wells which are applied to calculate the WCI. Red shaded box indicates hot source zone and black dots, triangular dots indicate pre-existed wells in WIC and wells located in hot source zone, respectively. 3 5

Figure 3-1. Initial distribution of (a) head and (b) TCE concentration. Cross dot indicate existing pumping well. Black box at (b) indicates TCE source zone with value of 1 mg/L..... 3 7

Figure 3-2. Pareto optimal front of NSGA-II at final generation with value of 100. Green solid line indicates the mean cost of all points. Blue and red line are set to $\pm 30\%$ boundaries of average cost, respectively. Point A, B, and C indicate optimal solutions at -30%, mean, and +30% costs..... 4 0

Figure 3-3. Best results of NSGA-II subject to (a) decreased cost (b) mean cost (c) increased cost; Head distribution. Black cross dots denote pre-existed pumping well and red cross dot indicates additional pumping well installs after optimization. 4 1

Figure 3-4. Best results of NSGA-II subject to (a) decreased cost (b) mean cost (c) increased cost; TCE concentration distribution. Black cross dots denote pre-existed pumping well, blue cross dot

<p>indicates additional pumping well installs after optimization and black box indicates TCE source zone.</p>	<p>4 2</p>
<p>Figure 3-5. Comparison of solutions using GA and NSGA-II. Blue dots indicate optimal solution sets obtained by NSGA-II and red star indicates optimal solution obtained by GA. Black solid line indicates the linear fit line for the Pareto optimal front.</p>	<p>4 5</p>
<p>Figure 3-6. Plot of objective function value versus generation number for each optimal solution obtained by GA.</p>	<p>4 6</p>
<p>Figure 3-7. Distribution of hydraulic conductivity at alluvial aquifer of WIC site.....</p>	<p>4 8</p>
<p>Figure 3-8. Initial concentration distribution of TCE in WIC. Black dots indicate observation well and black box indicate source zone of TCE.....</p>	<p>4 9</p>
<p>Figure 3-9. (a) Modeled head distribution of steady state flow. (b) modeled TCE concentration distribution with MT3D model. Black dots indicate observation wells and black box indicates TCE source zone.....</p>	<p>5 2</p>
<p>Figure 3-10. (a) Comparison between modeled and observed head with steady state groundwater flow. (b,c) Time series modeled and observed of head at GW-17 and concentration at KDPW-2 where located at hot source zone.....</p>	<p>5 3</p>
<p>Figure 3-11. Pareto optimal front in final generation. Blue and red dot indicate the different remediation scenarios.....</p>	<p>5 6</p>

Figure 3-12. Optimized simulation result at final time that is related to (a) first pump-and-treat scenario with the greatest decreasing of TCE (b) second pump-and-treat scenario with the greatest decreasing of TCE. 5 7

Figure 3-13. Total mass change of TCE depending on maximum cost in pump-and-treat scenarios. The black line indicates the total concentration change of the base model without pumping. The red and blue lines represent continuous and rainy season operation scenarios, respectively..... 5 8

Figure 3-14. Location of wells which contribute much to pump-and-treat subject to several scenarios. Blue labeled points, red labeled points, triangular point indicate contribute much for pump-and-treat only considered pumping rate, considered both specification of well and pumping rate, and well located in hot source zone, respectively. 6 1

LIST OF TABLES

Table 2-1. Parameters assigned in the benchmark model.....	1 2
Table 2-2. Constant parameters assigned in Wonju Industrial Complex (WIC) model.	1 7
Table 2-3. Measured groundwater head, hydraulic conductivity and the concentration of TCE at each observation well.....	2 1
Table 2-4. Data of well in WIC.	3 4
Table 3-1. Optimal pumping well locations and pumping rate for solutions selected in Figure 3-2. EP and AP are pumping rate for pre-existed, and additional pumping well, respectively.	4 3
Table 3-2. Calculation of the WCI for continuous operation.	6 2
Table 3-3. Calculation of the WCI for optimal pumping rate of rainy season operation.	6 3

1 INTRODUCTION

1.1 Research Background

Groundwater is a valuable water resource used for agricultural irrigation, drinking water, and as a geothermal heat exchanger for heat pump systems. Human activities in agricultural and industrial fields have a significant impact on the quality of groundwater, often resulting in groundwater contamination. Therefore, it is necessary to derive an effective strategy for the control and remediation of contaminated groundwater. Primarily, dry cleaning or car engineering factories of industrial complexes commonly utilize trichloroethylene(TCE) as a lubricant and an oil degreaser. However, contamination in soil and groundwater is occurring due to lack of proper management in continuous usage. TCE leakage causes severe groundwater contamination due to its toxicity and its ability to penetrate deep into groundwater (Jackson 1998; Rivett et al. 2001; Baek and Lee 2011). Therefore, from a groundwater remediation perspective, various technologies are suggested such as 1) physics-chemical based remediation, 2) biological based remediation and 3) natural attenuation, and these methods are adopted depending on site characteristics and contaminants reaction (Langwaldt and Puhakka 2000; Wang and Mulligan 2006; Reddy 2008; Lien et al. 2016). To identify an effective remediation technology for TCE in groundwater, a variety of groundwater remediation technologies had been applied to TCE contaminated areas (Moon et al. 2005; Rivett et al. 2006; Kim et al. 2007; Lee et al. 2007). Although a pump-and-treat method displays better effectiveness for TCE removal compared to other methods in an industrial complex (Lee et al. 2013), it has a limitation on a significant remediation costs and time. Therefore, there is a need to suggest cost-effective optimal remediation strategies to improve efficiency.

To enhance groundwater remediation efficiency, several optimization methods are applied to the contaminated groundwater site and then to find an optimal operation plan which can reduce remediation costs (Ahlfeld et al. 1988; Sawyer et al. 1995; Jeyakumar et al. 2007; D'Ambrosio et al. 2015). Mathematical programming such as Linear Programming (LP) or Non-Linear Programming (NLP) deals with convex or concave optimization problem. Especially, several theorems state that a strict convex optimization finds a unique optimal solution, known as global optimum (Bertsekas 2009). However, one of the disadvantages of mathematical programming is its requirement for significant computation time to solve optimization problem (Silveira et al. 2021). Additionally, it is often limited to specific forms of objective functions, which can restrict its applicability. To overcome these problems, meta-heuristic algorithm, such as Genetic Algorithm (GA), Particle Swarm Optimization (PSO), and Simulated Annealing (SA), is developed to solve optimization problem in groundwater remediation (McKinney and Lin 1994; Huang and Mayer 1997; Wang and Zheng 1999; Ko et al. 2005; Mategaonkar and Eldho 2012). McKinney and Lin (1994) evaluated the performance of GA in groundwater remediation problem and showed that GA is able to ferret out searching the global optimal solution and reduces computation time, compared to LP or NLP. Huang and Mayer (1997) stated that optimal well locations for pump-and-treat are sensitive variable to solve optimization problem in groundwater remediation. Although the meta-heuristic optimization algorithm presents better computation efficiency, local optimum which is pseudo optimal solution could be obtained (Beheshti and Shamsuddin 2013). Therefore, a realistic initialization of simulation should be coupled with the meta-heuristic optimization for improvement in searching the global optimum.

Previous studies couple the groundwater model with GA to suggest optimal operation design for pump-and-treat method (Ko et al. 2005; Park et al. 2007, 2011). Especially, Park et al. (2011) suggested optimal pump-and-

treat strategies in real groundwater contaminated site by coupling the groundwater model and GA. An application of GA in groundwater contaminated site only considers a single objective optimization problem, such as minimizing operation cost or operation time of remediation (Aly and Peralta 1999; Ko et al. 2005). Therefore, it is difficult to consider both cost and time with conventional approach. Furthermore, GA does not consider acceptable cost or target concentration in terms of remediation operation strategy. Therefore, there is a need for optimal solutions to multi-objective optimization problems, and many previous studies have coupled it with groundwater models that suggest optimal solutions (Erickson et al. 2002; Mondal et al. 2010; Singh and Chakrabarty 2010; Peralta 2012; Mirzaee et al. 2021). Peralta (2012) applied the weighting method that deals with multi-objective optimization problem. However, the weighting method requires lots of computational time to obtain optimal solution and does not guarantee that suggested solution is the global optimal solution (Konak et al. 2006; Asghar et al. 2015). To overcome limitations in the weighting method, Non-Dominated Sorting Genetic Algorithm-II (NSGA-II), which is based on GA and handles multi-objectives for optimization, is applied to solve optimization problems in groundwater remediation.

Recently, NSGA-II handles the groundwater remediation problem subject to various objectives (Mirzaee et al. 2021; Tabari and Abyar 2022; Zeynali et al. 2022). Mirzaee et al. (2021) solved nitrate contamination problem that maximizes economic benefits and minimizes the concentration of nitrate in groundwater. Zeynali et al. (2022) formulated objective function that handles not only cost and concentration but also drawdown and remediation time. Furthermore, an uncertainty of hydraulic and contaminant properties is an important factor for groundwater remediation (Teramoto et al. 2020; Yang et al. 2022). Yang et al. (2022) displayed that co-existing uncertainty of hydraulic conductivity and porosity should be considered to suggest optimal pump-and-treat strategies. Teramoto et al. (2020) showed that the fluctuation

of concentration subject to the water table is an important factor for the pump-and-treat method. However, these studies are limited on searching sensitive parameters such as pumping rate or operation time in the pump-and-treat methods. Furthermore, they do not suggest quantitative measurements of the importance of these parameters in wells. To reflect the conditions of contaminated site for pump-and-treat method, it is necessary to consider the integrated uncertainty that is existed at the contaminated site and propose an index related to pump-and-treat method. Moreover, solution sets obtained by multi-objective optimization could be applied for decision-making subject to groundwater remediation.

1.2 Objectives and Scope

The objective of this study applies a search-based Simulation-Optimization model to suggest the optimal design for the pump-and-treat method considering uncertainties (i.e. hydraulic conductivity, porosity, solute concentration) at TCE contaminated site. First, the benchmark model is established to evaluate the performance of multi-objective optimization and identify its applicability to the regional scale model. For alluvial aquifer model, the optimal design for the pump-and-treat method which considers the fluctuation of concentration caused by TCE trapped at the vadose zone is suggested. Consequently, in this study, the Well Contribution Index (WCI) that indicates the pumping rate and data of the well is proposed not only to suggest optimal remediation design considering site characteristics, but also to select the optimal pumping well which has priority for groundwater remediation.

2 METHODOLOGY

2.1 Site description

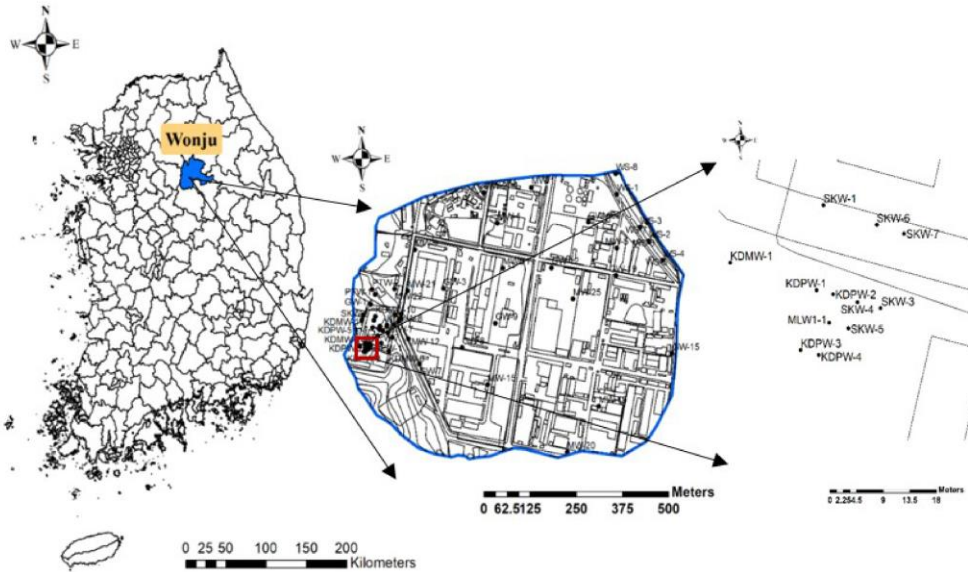
In this study, optimization of the pump-and-treat strategy is applied to one benchmark model and one regional scale study site: Wonju Industrial Complex (WIC) is highly contaminated at the alluvial aquifer.

WIC is located approximately 120 km away from Seoul, and southwestern part of Gangwon province (Figure 2-1). The left side of the study area has a higher elevation which is near Road Administrative Office (RAO), and the right side of the study area is near the Wonju stream. Geologically, the study area is composed of Jurassic biotite granite(Jbgr) and Quaternary alluvial deposits (Qa) (Figure 2-1). In addition, weathered rock and little fractured rock are included in bedrock aquifers (Korea water resources and corporation, 2011; Yang and Lee, 2012; Lee et al., 2013). In WIC, TCE is the main contaminant. RAO is highly contaminated by TCE, and hot source zone is located. Besides, it has been researched that several local TCE sources exist along the downstream direction from the RAO (Yang and Lee 2012). Due to the fact that there are main source and several local sources along groundwater flow direction that cause TCE contamination, groundwater remediation has been recognized as one of the major tasks to be carried out urgently in this area.

Figure 2-2 shows the concentration variation related to rainfall at the hot source zone. In this figure, the concentration of TCE is increased subject to rainfall. This is due to the fact that trapped TCE at the unsaturated zone is dissolved when the water table rises. In WIC, there is a positive correlation between hydraulic head variation and the concentration of TCE at the hot source zone (Yang and Lee 2012; Yang et al. 2012; Cho et al. 2020). To simulate the transport of TCE at WIC, concentration variation should be

considered, and mass loading at the source zone is assumed to show variation of TCE related to rainfall.

(a) Location of WIC



(b) Geological map of WIC

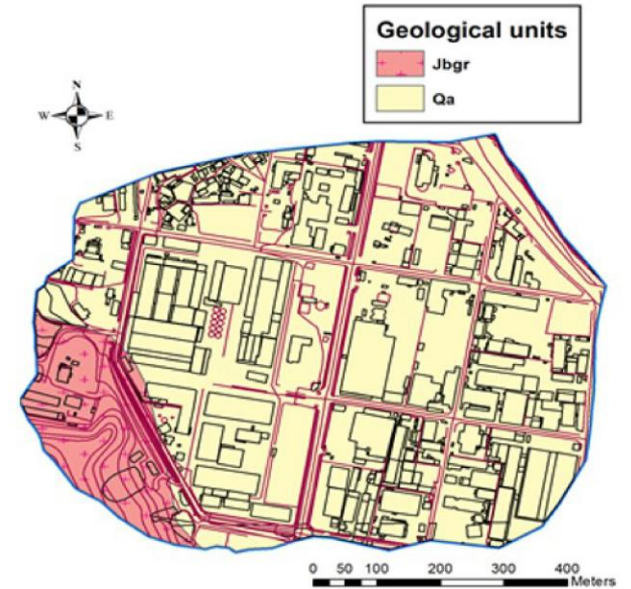


Figure 2-1. Site properties which are about (a) location and the source zone of the study area where is Woosan Industrial Complex (WIC) (b) Geological map of the study area. Red box indicates hot source zone and black dots indicate observation wells in this area. Qa and Jbgr indicate Quaternary alluvial deposits and biotite granite, respectively.

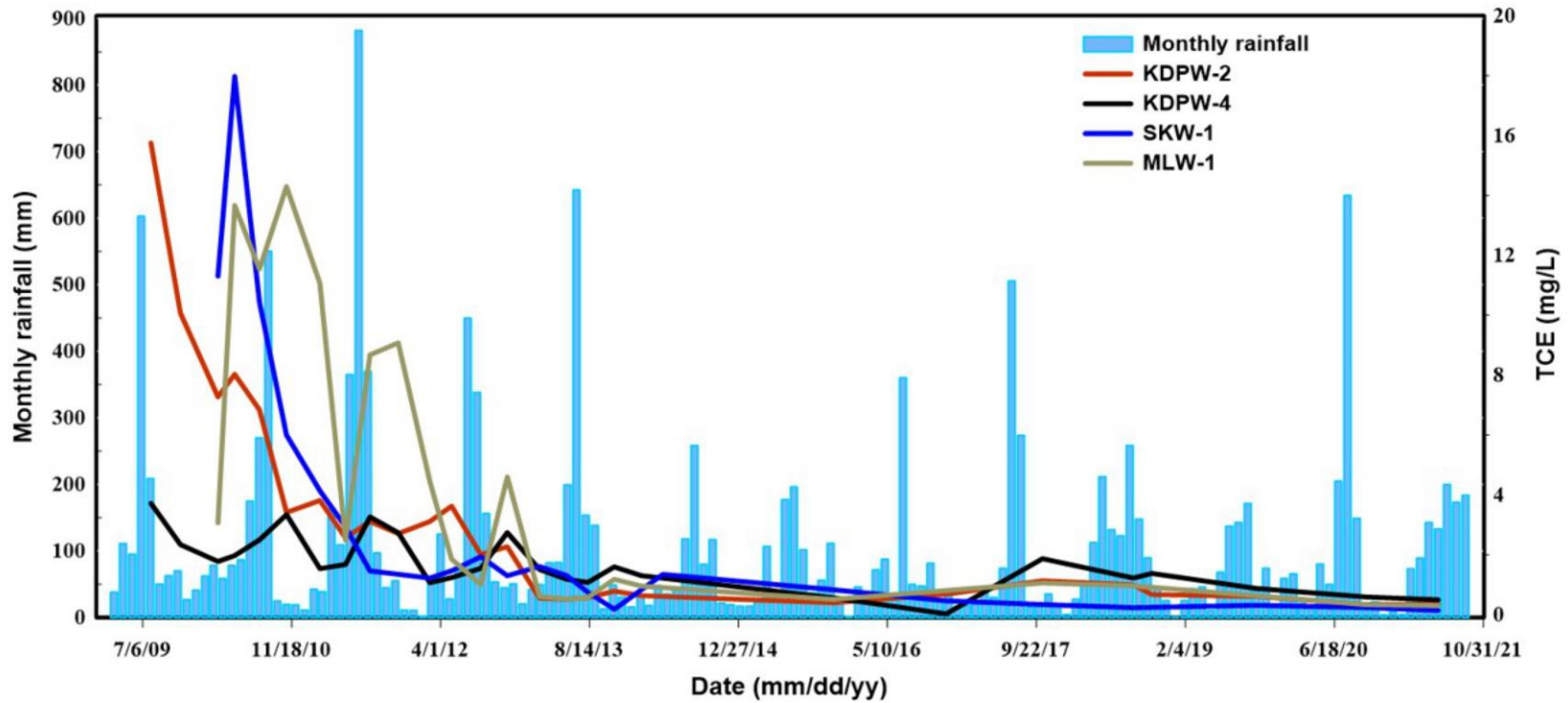


Figure 2-2. Monthly rainfall data and changes in TCE concentration at observation wells at Woosan Industrial Complex (WIC) site.

2.2 Numerical model

Two numerical models are adopted to simulate 1) groundwater flow and 2) dissolved phase of TCE transport. MODFLOW (Harbaugh 2005) is used to simulate groundwater flow, and MT3D (Zheng and Wang 1999) is used to simulate TCE transport.

2.2.1 MODFLOW

MODFLOW is widely used numerical model code that employs a finite difference method to solve a three-dimensional groundwater flow equation:

$$\frac{\partial}{\partial x} \left(K_{xx} \frac{\partial h}{\partial x} \right) + \frac{\partial}{\partial y} \left(K_{yy} \frac{\partial h}{\partial y} \right) + \frac{\partial}{\partial z} \left(K_{zz} \frac{\partial h}{\partial z} \right) - W = S_s \frac{\partial h}{\partial t} \quad (\text{Eq.2-1})$$

where K is hydraulic conductivity for each direction, h denotes hydraulic head, W is volumetric flux per unit volume which represents source and sink term, t is time, and S_s is specific storage. Source and sink term include recharge rate (i.e., rainfall), pumping or injection from wells, river, and drain. MODFLOW is modular simulator, and specific packages are activated to simulate groundwater flow. RCH package is used to input data related to recharge rate. WEL package is used to simulate pumping or injection of wells at specific location. RIV package enables to simulate interaction between groundwater and river, and requires head stage, bottom elevation, and conductance of each cell. The conductance of river (C_{riv}) is calculated using Eq.2-2.

$$C_{riv} = \frac{k_{riv} A}{L_{riv}} \quad (\text{Eq.2-2})$$

where L_{riv} is flow length, A is cross-sectional area of grid, and k_{riv} is hydraulic conductivity of river bottom.

Figure 2-3 shows brief description of benchmark problem with boundary

conditions, including constants head, no flow boundary, and pumping or injection wells. Analysis of benchmark problem is performed to identify whether optimal pump-and-treat design could be simulated. Benchmark problem assumes a rectangular shaped domain (4500 m × 5000 m) and the size of grid is 250 m × 250 m. In this model, constant head boundaries are assigned at upper and lower boundary, and no flow boundaries are assigned at left and right side of model domain. Also, there are two pumping wells with 1000 m³/day, and these pumping rates are reduced to a quarter of current state for searching optimal pumping rate. At initial state, TCE source zone with a concentration of 1 mg/L is assigned to the right upper side of the model domain, while the rest of the area has no TCE contamination. Table 2-2 shows parameters used in benchmark analysis. Upper and lower boundary assigned as specified head boundaries to show direction of groundwater flow. A simulation time of benchmark problem is 1820 days (≈5 years).

A regional scale model of WIC consists of 19,474 horizontal grids, and two vertical layers that include an alluvial at top and a bedrock layer at bottom (Figure 2-4). The horizontal fine grid is adopted near observation wells. For boundary conditions, specified head boundary is assigned in the left side of the model and the right side of the model boundary is assigned as a river boundary (Figure 2-5). Rest of boundaries are set as no-flow boundary.

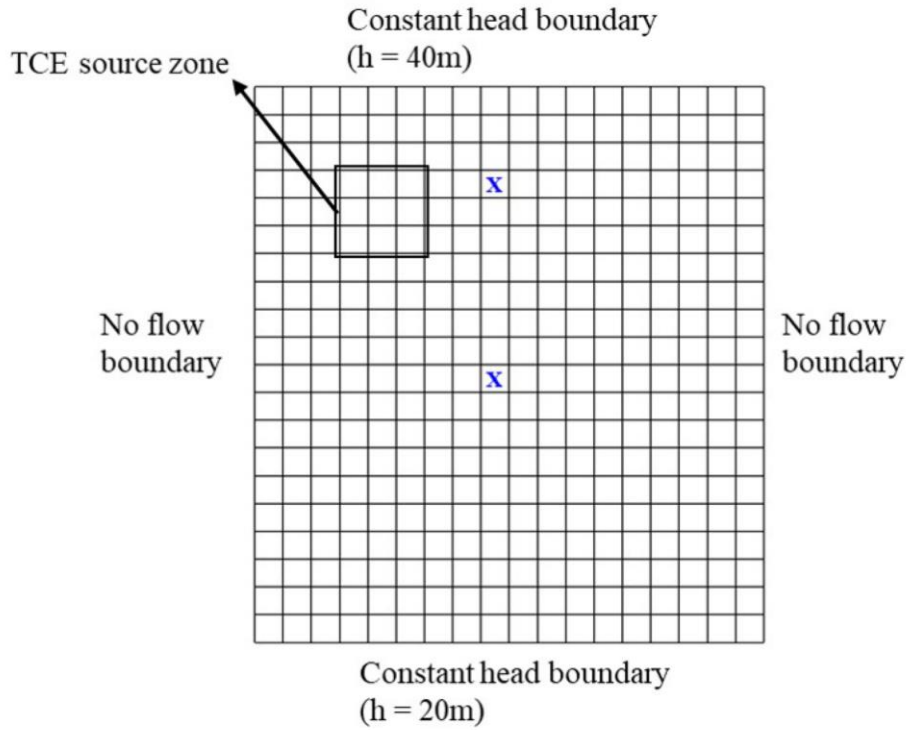


Figure 2-3. Model domain and boundary conditions for benchmark problem. Blue cross dots indicate the location of pumping wells. Black rectangular box is TCE source zone.

Table 2-1. Parameters assigned in the benchmark model.

Parameter	Value
Hydraulic Conductivity (cm/sec)	1.2×10^{-2}
Recharge rate (m/day)	5.0×10^{-5}
Longitudinal Dispersivity (m)	10
Transverse Dispersivity (m)	1
Pumping rate for pre-existed well (m ³ /day)	1000

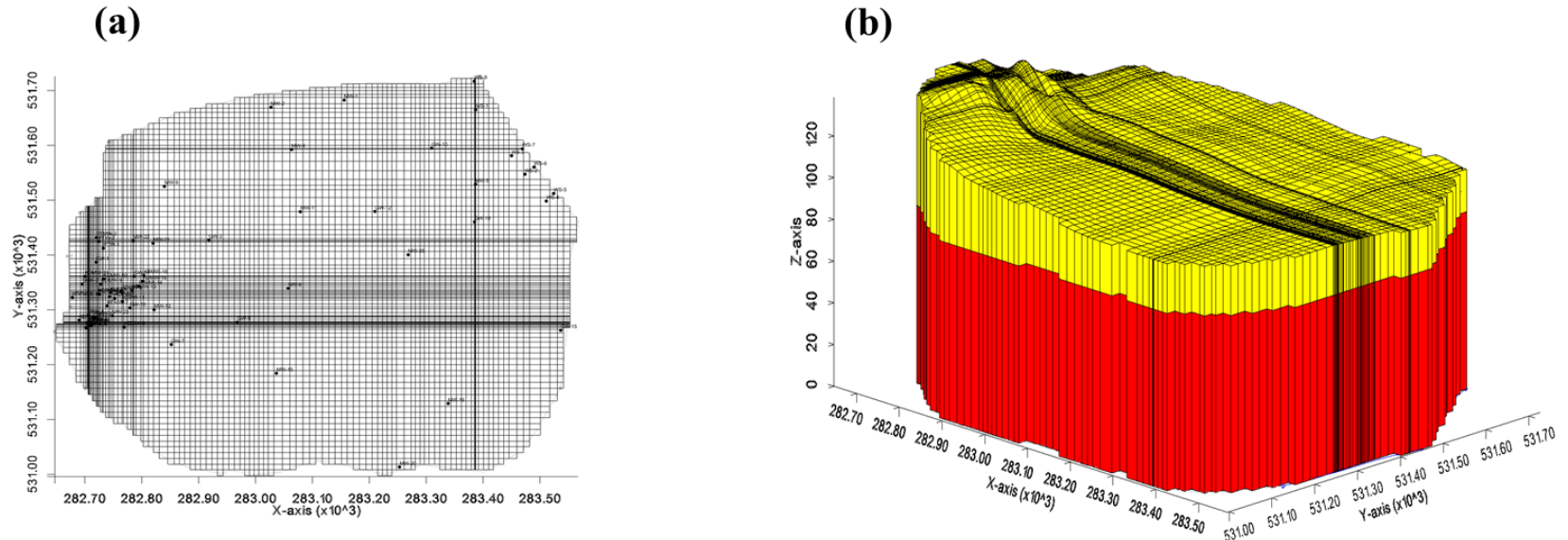


Figure 2-4. Model grid and boundary conditions for Wonju Industrial Complex (WIC); (a) Model grid design for horizontal direction. (b) Model grid design for vertical direction. Black dots in (a) indicate observation wells. Yellow and red color in (b) indicate alluvial and bedrock layer, respectively.

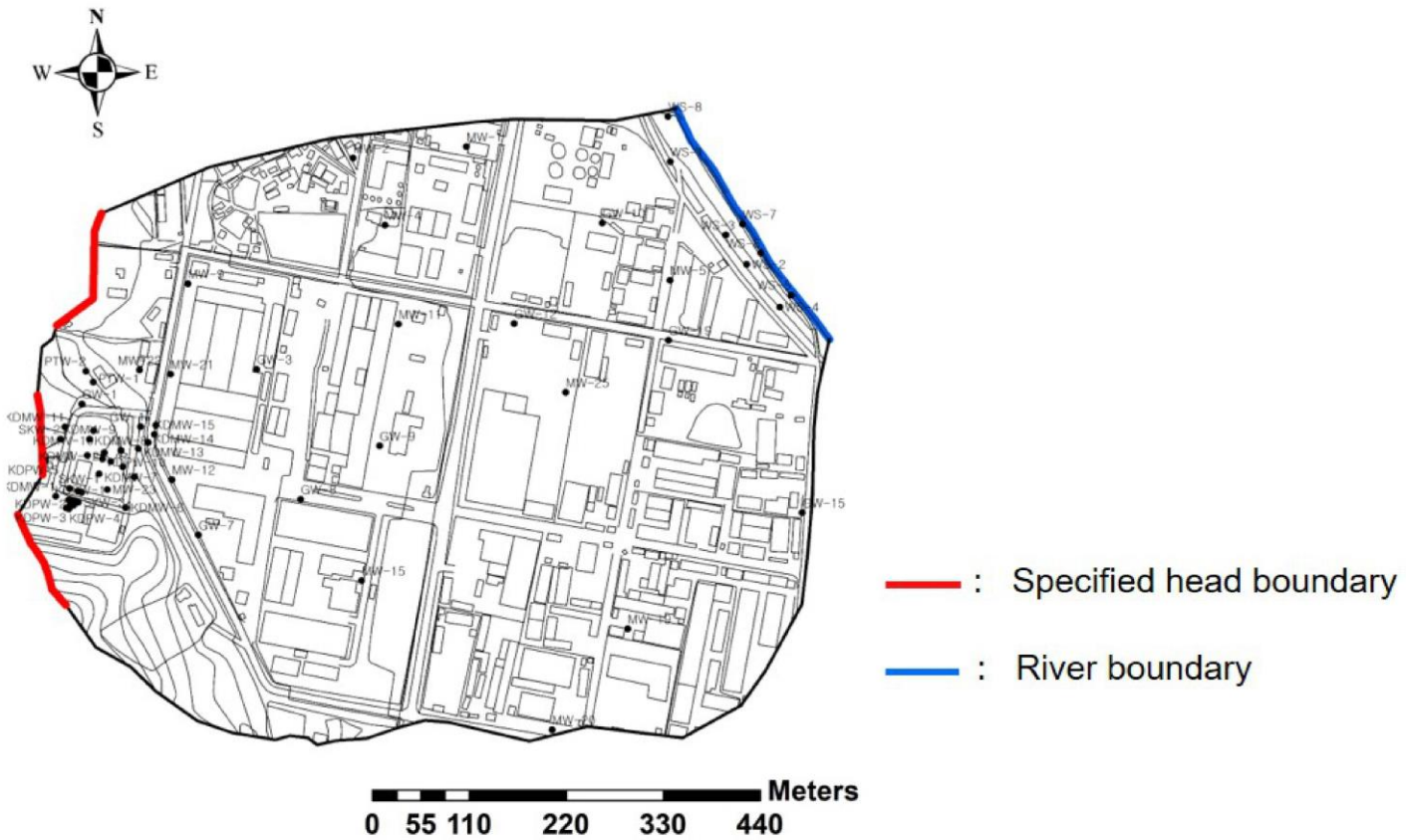


Figure 2-5. Boundary conditions assigned for groundwater flow model in WIC.

2.2.2 MT3D

MT3D is one of the solute transport model coupled with MODFLOW. The three-dimensional solute transport is expressed as follows:

$$\frac{\partial(\theta C^k)}{\partial t} = \frac{\partial}{\partial t} \left(\theta D_{ij} \frac{\partial C^k}{\partial x_j} \right) - \frac{\partial}{\partial x_i} (\theta v_i C^k) + q_s C_s^k + \sum R_n \quad (\text{Eq.2-3})$$

where C^k is the concentration of dissolved k species, D is dispersion coefficient, v is linear pore water velocity, θ is porosity, q_s is the mass transfer rate, C_s^k is the concentration of the source or sink flux for k species, R_n is chemical reaction including sorption and decay and given by

$$\sum R_n = -\rho_b \frac{\partial \bar{C}^k}{\partial t} - \lambda_1 \theta C^k - \lambda_2 \rho_b \bar{C}^k \quad (\text{Eq.2-4})$$

where ρ_b is the bulk density, \bar{C}^k is the sorbed concentration of species k, and λ is the first-order reaction rate for the dissolved and sorbed phase. MT3D is also modular simulator, therefore, several packages are required to active. ADV and DSP packages are used to simulate advection and dispersion, respectively. To improve computation efficiency, a Third-order total Variation Diminishing (TVD) is used. A dispersion coefficient (D) of solution transport includes mechanical dispersion and molecular diffusion is given by

$$\begin{aligned} D_{xx} &= \alpha_L \frac{v_x^2}{|v|} + \alpha_{TH} \frac{v_y^2}{|v|} + \alpha_{TV} \frac{v_z^2}{|v|} + D^* \\ D_{yy} &= \alpha_L \frac{v_y^2}{|v|} + \alpha_{TH} \frac{v_x^2}{|v|} + \alpha_{TV} \frac{v_z^2}{|v|} + D^* \\ D_{zz} &= \alpha_L \frac{v_z^2}{|v|} + \alpha_{TH} \frac{v_x^2}{|v|} + \alpha_{TV} \frac{v_y^2}{|v|} + D^* \end{aligned} \quad (\text{Eq.2-5})$$

where D is dispersion tensor, α_L is longitudinal dispersivity, α_T is transverse dispersivity along with horizontal (H) and vertical direction (V),

D^* is effective molecular diffusion coefficient, v is the component of the velocity vector. To estimate mass removal after remediation, total mass of contaminant $M(t)$ at specific time is calculated.

$$M(t) = \sum_{i=1}^{n_{grid}} (H_i^{top} - H_i^{bottom}) \times A_i \times \theta_i \times C_i(t) \quad (\text{Eq.2-6})$$

where $M(t)$ is the mass of contaminant at specific time, and n_{grid} is number of grid, H^{top} and H^{bottom} are a height of top and bottom elevation of specific grid. A is area of grid, θ is porosity, $C(t)$ is the concentration at specific time. TCE is a by-product of tetrachloroethylene (PCE) dechlorination (Figure 2-6). A first-order irreversible decay reaction is considered and Eq.2-7 includes dechlorination term for chlorinated solvent which expressed as form of matrix equation.

$$\begin{aligned} \begin{bmatrix} R_1 & 0 \\ 0 & R_2 \end{bmatrix} \begin{bmatrix} \frac{\partial c_1}{\partial t} \\ \frac{\partial c_2}{\partial t} \end{bmatrix} + \begin{bmatrix} v \frac{\partial c_1}{\partial x} \\ v \frac{\partial c_2}{\partial x} \end{bmatrix} - \begin{bmatrix} D_x \frac{\partial^2 c_1}{\partial x^2} \\ D_x \frac{\partial^2 c_2}{\partial x^2} \end{bmatrix} - \begin{bmatrix} D_y \frac{\partial^2 c_1}{\partial y^2} \\ D_y \frac{\partial^2 c_2}{\partial y^2} \end{bmatrix} - \begin{bmatrix} D_z \frac{\partial^2 c_1}{\partial z^2} \\ D_z \frac{\partial^2 c_2}{\partial z^2} \end{bmatrix} \\ = \begin{bmatrix} -k_1 & 0 \\ 0 & -k_2 \end{bmatrix} \begin{bmatrix} c_1 \\ c_2 \end{bmatrix} \end{aligned} \quad (\text{Eq.2-7})$$

where c_1 and c_2 are a concentration of PCE and TCE, respectively. R is a retardation factor of PCE and TCE. k_1 is decay rate of PCE and k_2 is decay rate of TCE.

Table 2-2 shows parameters spatially assigned in the model. The storativity is estimated with a hydraulic test in this study site. Both dispersivity and decay rate are assigned from literature-based values.

Table 2-2. Constant parameters assigned in Wonju Industrial Complex (WIC) model.

Parameter	Value
Specific yield in layer 1 (-)	0.1
Specific storage in layer 1 (m^{-1})	1.0×10^{-4}
Specific yield in layer 2 (-)	0.05
Specific storage in layer 2 (m^{-1})	1.0×10^{-5}
Longitudinal dispersivity (m)	10
Transverse dispersivity (m)	1
Decay rate (day^{-1})	5.0×10^{-4}

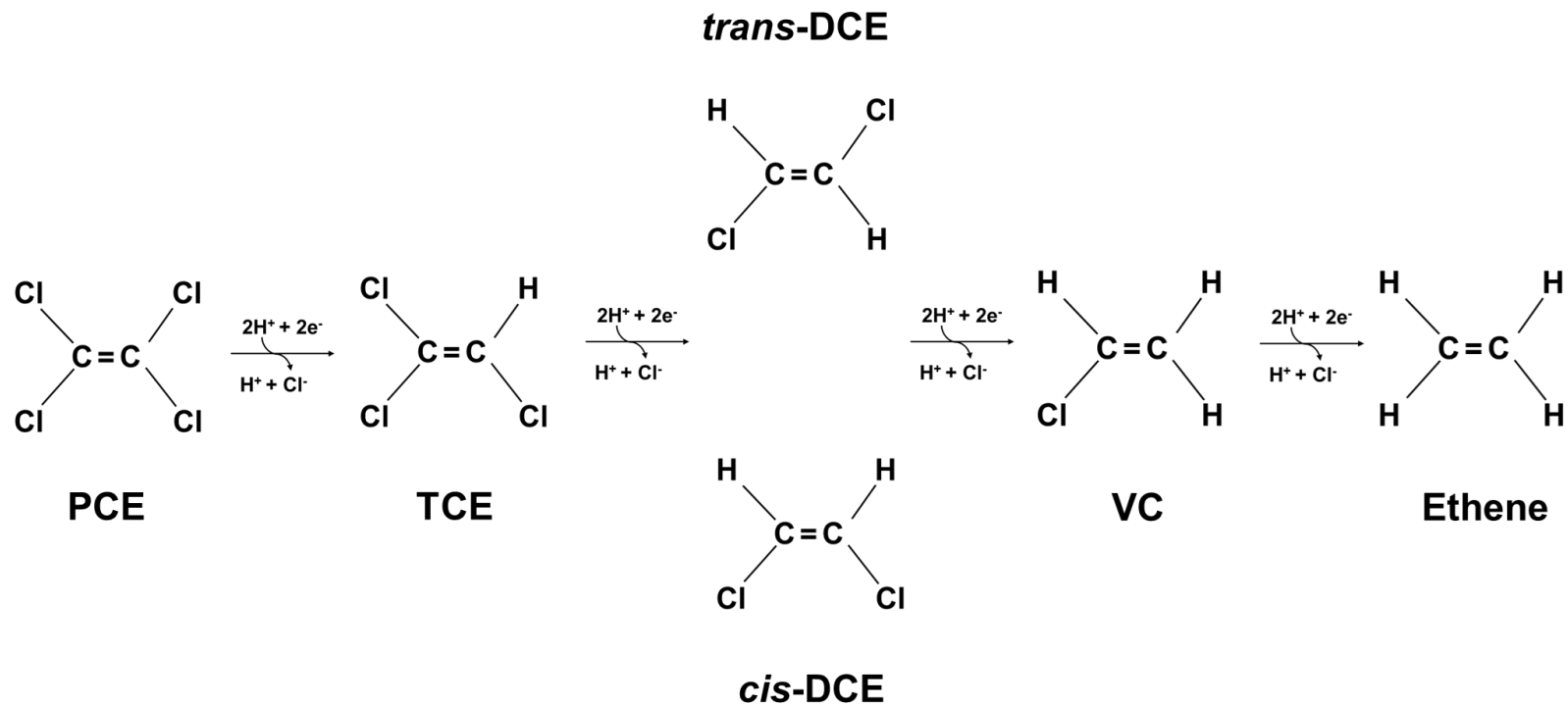


Figure 2-6. Chemical reaction procedure of PCE and TCE.

2.3 Geostatistical model

A geostatistical model is generally used to generate heterogeneity in aquifers, such as hydraulic conductivity and specific storage coefficient, and concentration distribution of solute. Here, kriging and Inverse Distance Weighting (IDW) are used to generate the heterogeneous hydraulic conductivity field, and initial concentration distribution of TCE, respectively.

2.3.1 Kriging

Kriging is used to predict value at specific points using linear weighting combination with known value (Choe 2013). Eq.2-8 is an equation that applied the simple kriging method to predict unknown value and Eq.2-9 is an equation that shows the relationship between variance of error and covariance.

$$z^* = \sum_{i=1}^n \lambda_i z_i \quad (\text{Eq.2-8})$$

$$\sigma^2_{SK} = \text{Var}(z) - 2\text{Cov}(z, z^*) + \text{Var}(z^*) \quad (\text{Eq.2-9})$$

where z^* is unknown value at specific point, λ_i is weight and z_i is known value, σ^2_{SK} is error variance, $\text{Var}(z)$ is a variance function of known value, $\text{Var}(z^*)$ is a variance function of predicted value, and $\text{Cov}(z, z^*)$ is a covariance function estimated with spatial distance. A strong constraint on the simple kriging is that sum of weights is equal to one, therefore, the simple kriging derives biased predicted values (Choe 2013). Due to this shortcoming of the simple kriging, the ordinary kriging is applied to minimize the bias for predicted value and variance of error. Ordinary kriging employs a form of Lagrangian equation that minimizes error in variance. As minimizes the error in variance, the ordinary kriging suggests a more reliable predicted value, compared to the simple kriging. The equation of the ordinary kriging is given as

$$L(\lambda_1, \lambda_2, \dots, \lambda_n; w) = \sigma^2 - 2 \sum_{i=1}^n \lambda_i \sigma^2_{0i} + \sum_{i=1}^n \sum_{j=1}^n \lambda_i \lambda_j \sigma^2_{ij} + 2w(1 - \sum_{i=1}^n \lambda_i) \quad (\text{Eq.2-10})$$

where L is the lagrangian objective function, w is a Lagrange factor, and σ is the variance of error in each factor. The ordinary kriging requires a semi-variogram model, therefore, a spherical model is applied in this study:

$$\gamma(h) = \begin{cases} C_0 \left[1.5 \left(\frac{h}{a} \right) - 0.5 \left(\frac{h}{a} \right)^3 \right], & h \leq a \\ C_0, & h > a \end{cases} \quad (\text{Eq.2-11})$$

where C_0 is nugget value, a is correlation distance, and h is spatial distance. The nugget value is 0.103, the range is 79.3 m and the partial sill is 1.84. A point value of hydraulic conductivity and concentration is described in Table 2-3. The value of hydraulic conductivity is obtained by the slug test performed in this study site.

Table 2-3. Measured groundwater head, hydraulic conductivity and the concentration of TCE at each observation well.

Coordinate system: EPSG 5186

Well	X	Y	Head (m)	K (cm/sec)	TCE (mg/L)
GW-1	282,720.00	531,386.71	123.20	1.60E-04	0.024
GW-3	282,918.22	531,426.64	108.69	2.26E-03	0.510
GW-7	282,852.23	531,236.46	112.64	3.53E-04	0.006
GW-8	282,968.22	531,277.39	107.80	1.44E-02	0.060
GW-9	283,057.72	531,338.98	107.03	1.29E-03	0.088
GW-10	283,310.08	531,594.57	104.31	1.31E-02	0.095
GW-12	283,210.18	531,479.24	105.13	6.80E-04	0.2
GW-17	282,786.51	531,360.84	115.09	2.05E-04	0.001
GW-19	283,385.22	531,459.91	104.67	6.17E-03	0.079
MW-2	283,027.54	531,669.21	107.99	1.09E-03	0.003
MW-4	283,063.72	531,592.17	107.10	6.02E-04	0.016
MW-5	283,386.95	531,528.92	104.49	1.56E-02	0.004
MW-9	282,840.11	531,524.85	108.68	1.76E-03	0.104
MW-11	283,079.01	531,478.60	106.70	1.24E-03	0.341
MW-12	282,821.99	531,300.06	114.72	5.96E-03	0.221
MW-15	283,037.00	531,184.26	107.67	5.70E-04	0.001
MW-21	282,820.32	531,421.13	109.26	2.40E-03	0.271
MW-22	282,785.29	531,425.81	109.81	9.59E-04	0.097
MW-23	282,748.74	531,288.77	126.68	1.43E-04	0.013
KDMW-1	282,690.37	531,281.06	126.50	2.76E-04	0.386

Table 2-3. Continued.

Well	X	Y	Head (m)	K (cm/sec)	TCE (mg/L)
KDMW-2	282,721.84	531,242.66	134.62	6.21.E-05	0.004
KDMW-4	282,627.41	531,269.07	128.28	1.74.E-04	0.003
KDMW-6	282,769.52	531,268.06	116.67	2.63.E-05	0.040
KDMW-7	282,739.49	531,306.63	125.68	3.51.E-04	0.435
KDMW-8	282,764.54	531,333.87	117.10	8.74.E-05	0.319
KDMW-9	282,728.68	531,346.48	123.92	1.32.E-04	0.177
KDMW-10	282,733.26	531,356.08	116.52	5.24.E-04	0.154
KDMW-11	282,700.40	531,360.73	125.04	7.13.E-03	0.024
KDMW-12	282,745.43	531,331.04	121.12	4.90E-04	0.030
KDMW-13	282,783.92	531,335.61	119.41	5.82E-05	0.376
KDPW-2	282,707.76	531,276.17	126.32	4.17.E-04	2.005
KDPW-4	282,705.32	531,266.80	127.16	1.50.E-04	1.547
KDPW-5	282,678.37	531,322.31	125.73	1.54.E-04	0.017
KDPW-6	282,761.82	531,383.65	125.20	1.22.E-03	0.124
KDPW-7	282,752.59	531,320.85	120.34	8.75.E-05	0.394
KDPW-8	282,725.99	531,328.17	125.08	3.16.E-04	1.059
KDPW-10	282,743.53	531,323.80	122.71	8.59E-05	0.043
KDPW-11	282,766.39	531,315.04	117.69	6.41E-06	0.375
MLW1-1	282,707.10	531,271.79	126.67	1.24.E-04	1.005
MLW1-2	282,707.07	531,271.70	126.75	9.30.E-04	0.318
MLW1-3	282,707.14	531,271.66	126.36	1.26.E-03	0.787

Table 2-3. Continued.

Well	X	Y	Head (m)	K (cm/sec)	TCE (mg/L)
SKW-3	282,715.77	531,274.03	126.60	3.46.E-04	0.386
SKW-4	282,711.85	531,274.95	126.28	4.99.E-04	0.225
SKW-6	282,715.14	531,286.89	126.14	2.40.E-03	2.650
SKW-7	282,719.73	531,285.52	126.02	3.37.E-03	0.637
PTW-1	282,732.70	531,412.09	113.35	9.55.E-05	0.022
PTW-2	282,724.55	531,424.71	113.29	2.94.E-04	0.030

2.3.2 Inverse Distance Weighting (IDW)

Kriging has a shortcoming in that predicted value converges to the average value which indicates variance is minimized (Choe 2013). For example, some solutes such as TCE and other contaminants, is limited in specific area or points and scarcely observed in non-leaked place. However, an application of the kriging in these concentration data generates non-zero concentration in non-leaked areas. On the other hand, IDW is one of the alternative interpolation methods to overcome shortcomings in concentration data, and is applied to estimate initial concentration distribution of TCE. IDW is the other geostatistical model which estimates unknown values using estimated values. In contrast to kriging, IDW does not require a semi-variogram model, and weight is estimated as inversely proportional to distance (Choe 2013). Eq.2-12 is used to calculate weight in IDW. Due to its properties, values near observed value show higher accuracy. However, IDW does not include spatial correlation and difference.

$$\lambda_i = \frac{\left(\frac{1}{d_i}\right)^\alpha}{\sum_{j=1}^n \left(\frac{1}{d_j}\right)^\alpha} \quad (\text{Eq.2-12})$$

where λ_i is weight, and d is distance between observed and predicted value.

2.4 Optimization for pump-and-treat

A meta-heuristic optimization algorithm is an iterative method that is applied to reduce the computation time for searching optimal solutions. Especially, metaheuristic optimization solves the objective function that subjects to restrictive space (Silveira et al. 2021) and evolutionary algorithm, such as Genetic Algorithm (GA) or Simulated Annealing (SA). In this study, NSGA-II is used to deal with multi-objective optimization problems consider reducing both costs and concentration.

NSGA-II considers an elitism and sorting process, and enhances computational speed in solving multi-objective optimization problems, compared to other evolutionary algorithms. NSGA-II is based on a genetic algorithm scheme that involves several key procedures, including generation, mutation, and crossover. Additionally, it incorporates non-dominated sorting and crowding distance sorting as its main procedures. (Figure 2-7). The crossover means that numbers in the other two strings are exchanged (Figure 2-7a). The mutation means that the number in one string is changed within a certain probability (Figure 2-7b). The non-dominated sorting is to sort population in order of level of non-domination and domination expresses differently from other cases (Deb et al. 2002; Yusoff et al. 2011). The crowding distance is to calculate the distance between populations in the Pareto front, and maintains a diversity of solutions in the population at each generation.

In the first generation of NSGA-II, the population is randomly generated, and the values of two objectives are calculated using the numerical model (Figure 2-8). To generate the next step generation (referred to “children”), the crossover and mutation procedures are sequentially applied to the previous population (referred to “parents”). Once the children are generated, both children and parents are merged. The non-dominated is then applied to rank

the merged population, and crowding-distance sorting is used to select the same number of parents' population from the merged population.

The best non-dominated solution set has a priority in selection. Figure 2-8 shows the brief procedure of Simulation-Optimization (S-O) modeling with NSGA-II. As the population is evolved, Pareto front is generated at each generation. A final generation shows the Pareto optimal front which is optimal solution set in the multi-objective optimization problem. Theoretically, it would be near to the global optimal solution, but reliable initial condition could generate the global optimal solution.

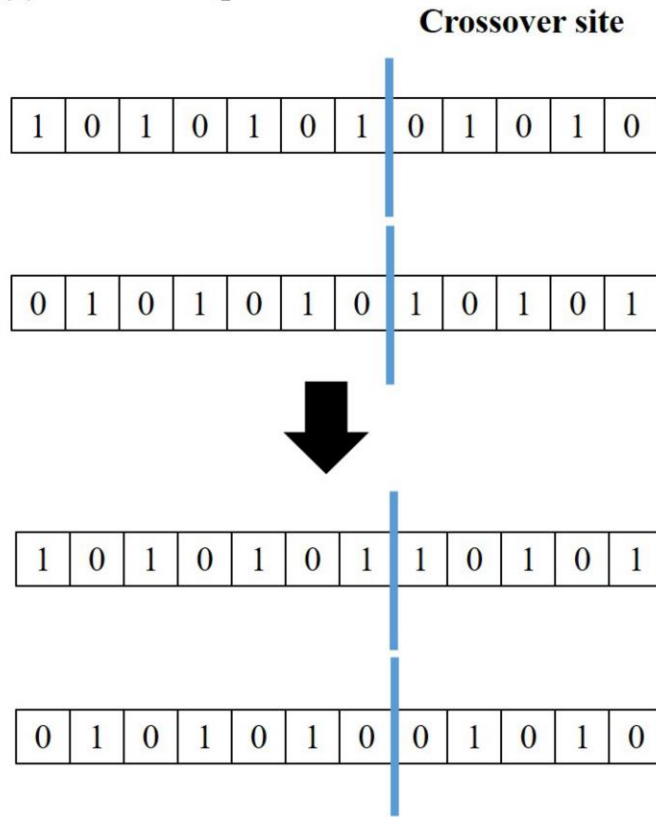
Here, the multi-objective function in NSGA-II focuses on minimizing both the cost of operating pump-and-treat and mass at the end of the simulation. The total concentration mass could be calculated with concentration at specific wells, and includes the same objective of reducing the concentration. Multi-objective functions are given by

$$\text{Minimize Cost} = n_{\text{wel}} \text{ Cost}_{\text{inst}} + a_{\text{pmp}} \sum_{i=1}^{n_{\text{wel}}} Q_i(t) \times t_{\text{fin}} \quad (\text{Eq.2-13})$$

$$\text{Minimize Concentration} = \sum_{i=1}^{n_{\text{wel}}} C_i(t_{\text{end}}) \quad (\text{Eq.2-14})$$

where n_{wel} is number of wells, $\text{Cost}_{\text{inst}}$ is cost for additional installation of one pumping well, a_{pmp} is the operation of pumping well cost, $Q(t)$ is pumping rate at specific time, t_{fin} is operation time, and $C(t_{\text{end}})$ is the concentration at specific point at end of simulation time.

(a) Crossover operator



(b) Mutation operator

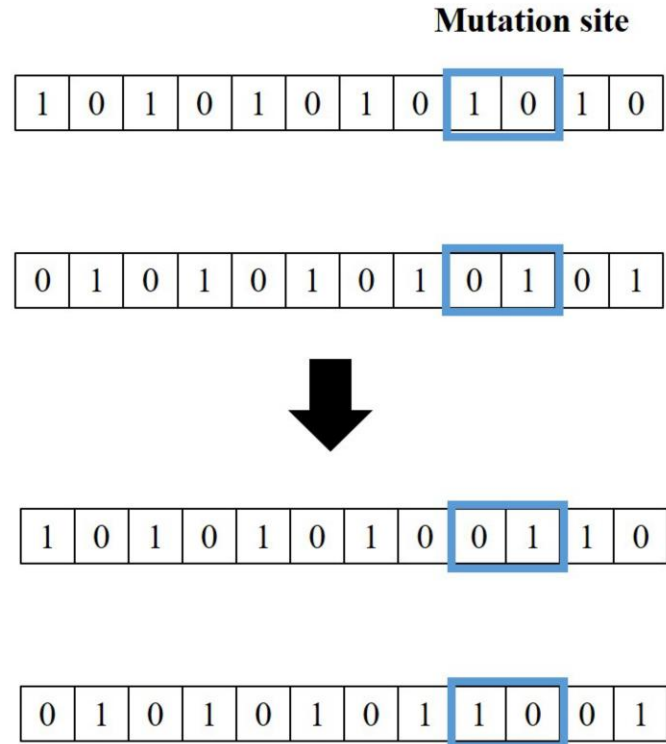


Figure 2-7. (a) Crossover and (b) Mutation operators

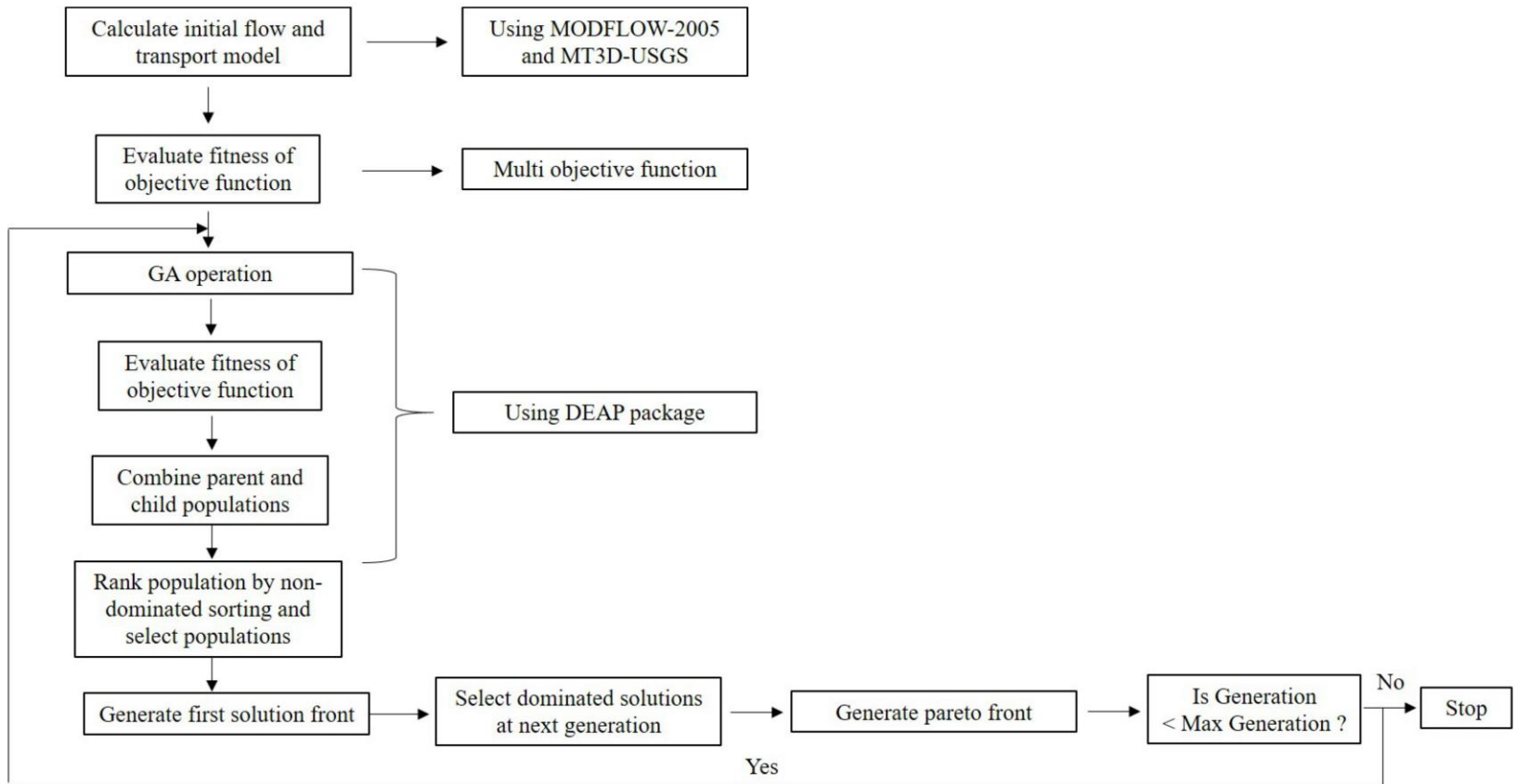


Figure 2-8. Flowchart of Simulation coupled with optimization modeling that uses NSGA-II for optimization.

2.5 Relative performance assessment

In the evaluation of the performance of meta-heuristic optimization algorithms, criteria such as effectiveness, efficiency, and reliability are commonly considered (Maier et al., 2014). The performance assessment involves comparing the relative effectiveness and efficiency of different algorithms, such as GA and NSGA-II.

GA has been widely used and has shown good performance in solving optimization problems related to groundwater remediation (McKinney and Lin 1994; Wang and Zheng 1999). Therefore, in the performance assessment, the relative Effectiveness (EF) and Efficiency (EY) of NSGA-II can be evaluated by comparing them to GA. This comparison allows us to understand how well NSGA-II performs in relation to GA.

To assess the EF, the convergence of GA can be examined, indicating how close its solutions are to the global optimal solution. For NSGA-II, the obtained pareto front can be compared to the optimal solution obtained by GA to evaluate its effectiveness. EY is evaluated based on the elapsed time taken by each algorithm to find optimal solutions. A faster algorithm is considered more efficient in finding solutions.

In this study, the performance of NSGA-II is evaluated using the global optimal solutions obtained by GA. Optimal solutions obtained by GA serve as a benchmark to assess the EF and EY of NSGA-II. Figure 2-9 is a flowchart that illustrates the process of relative performance assessment for GA and NSGA-II. It highlights the evaluation of EF and EY using the approaches mentioned above.

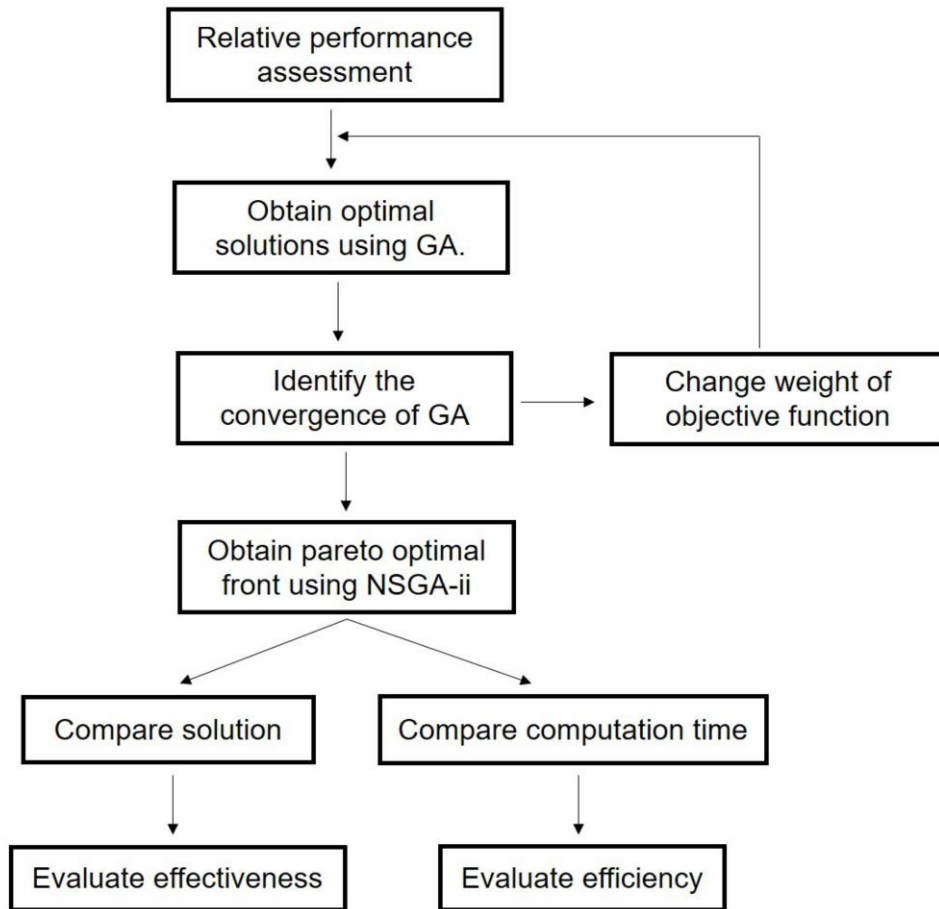


Figure 2-9. Flowchart of relative performance assessment for NSGA-II.

2.6 Factors of optimal pump-and-treat

The Well Contribution Index (WCI) is determined by utilizing optimal solutions obtained from multi-objective optimization and considering site characteristics that are relevant to pump-and-treat operations. Various data related to each well, such as the length of well screen, casing, and depth, are taken into account during the calculation process. By using the Pareto optimal front, it becomes possible to estimate the variation in pumping rates for each well based on the corresponding concentration, which serves as a measure of the remediation effect. Table 2-3 provides the well data for the Wonju Industrial Complex (WIC), and Eq.2-15 is applied to compute the WCI for each well. In this equation, the weights assigned to each factor sum up to 1, as described in Eq.2-16. The WCI is calculated for a total of 18 observation wells in the WIC, and the locations of these wells can be observed in Figure 2-9. The selection of these specific wells was based on the findings obtained from the TCE transport analysis conducted using the base model.

$$WCI = \sum a_x P_x \quad (\text{Eq.2-15})$$

$$\sum a_x = 1 \quad (\text{Eq.2-16})$$

where a_x is the weighting for each item and P_x is the score for each item. In the calculation of the Well Contribution Index (WCI), several factors should be considered based on the data of wells in the Wonju Industrial Complex (WIC). These factors include:

Factor 1: Length of screen

A longer well screen allows for increased contact area with the aquifer, resulting in more efficient water extraction. Wells with longer screen have a higher potential to contribute to effective groundwater remediation. Therefore,

a higher index score and weight can be assigned to wells with longer screen lengths.

Factor 2: Depth of the well

The concentration of DNAPL (dense non-aqueous phase liquid) generally increases with depth. However, in the case of the WIC, studies have shown a decrease in TCE concentration with depth (Yang et al. 2012). Wells with greater depth may have lower TCE concentrations and thus can be assigned a higher index score and lower weight.

Factor 3: Diameter of the well

Larger well diameters allow for the use of different types of pumps in pump-and-treat operations, which can affect the efficiency of water extraction. Wells with larger diameters can be assigned a higher index score and lower weight.

Considering these factors, the WCI calculation takes into account the specific characteristics of each well in terms of its length of screen, depth, and diameter. The assigned index scores and weights reflect the importance of these factors in determining the potential contribution of each well to effective groundwater remediation.

Taking into account the specific conditions of the WIC site, two scenarios are considered for the calculation of the WCI. The first scenario involves continuous extraction of groundwater from the wells throughout the simulation period, while the second scenario considers extraction only during the rainy season between June and August from 2009 to 2014. This seasonal extraction accounts for the effect of rainwater infiltration through the vadose zone, which can dissolve trapped TCE and result in higher TCE concentrations in groundwater during the rainy season. The operation time for both scenarios is set to 450 days, and the cost is proportional to the

pumping rate. This approach takes into consideration previous pilot tests of pump-and-treat conducted in the WIC, as described in the studies by Lee et al. (2013) and Jeon et al. (2013). By evaluating the WCI based on these factors and scenarios, the most effective wells for groundwater remediation can be identified.

Table 2-4. Data of well in WIC.

Well	X	Y	Depth of well (m)	Length of screen (m)	Well diameter (inch)
KDMW-7	282739.5	531306.6	21	15	4
MW-23	282748.7	531288.8	20	12	2
KDMW-6	282769.5	531268.1	24	18	4
GW-7	282852.2	531236.5	24	13.5	2
MW-12	282822	531300.1	9.4	7.5	2
GW-18	282779.4	531303.4	17	12	2
KDPW-11	282766.4	531315	21	16	2
KDPW-7	282752.6	531320.8	30	24	4
KDPW-10	282743.5	531323.8	30	25	4
KDPW-8	282726	531328.2	28.5	22.5	4
KDMW-9	282728.7	531346.5	27	21	4
KDMW-10	282733.3	531356.1	27	21	4
KDMW-12	282745.4	531331	27	22	2
KDMW-8	282764.5	531333.9	28	22	4
KDMW-13	282783.9	531335.6	30	25	3
KDMW-14	282795.1	531342.7	10	8	2
KDMW-15	282802.3	531352	14	12	2
KDMW-16	282803.8	531362.6	14	12	2

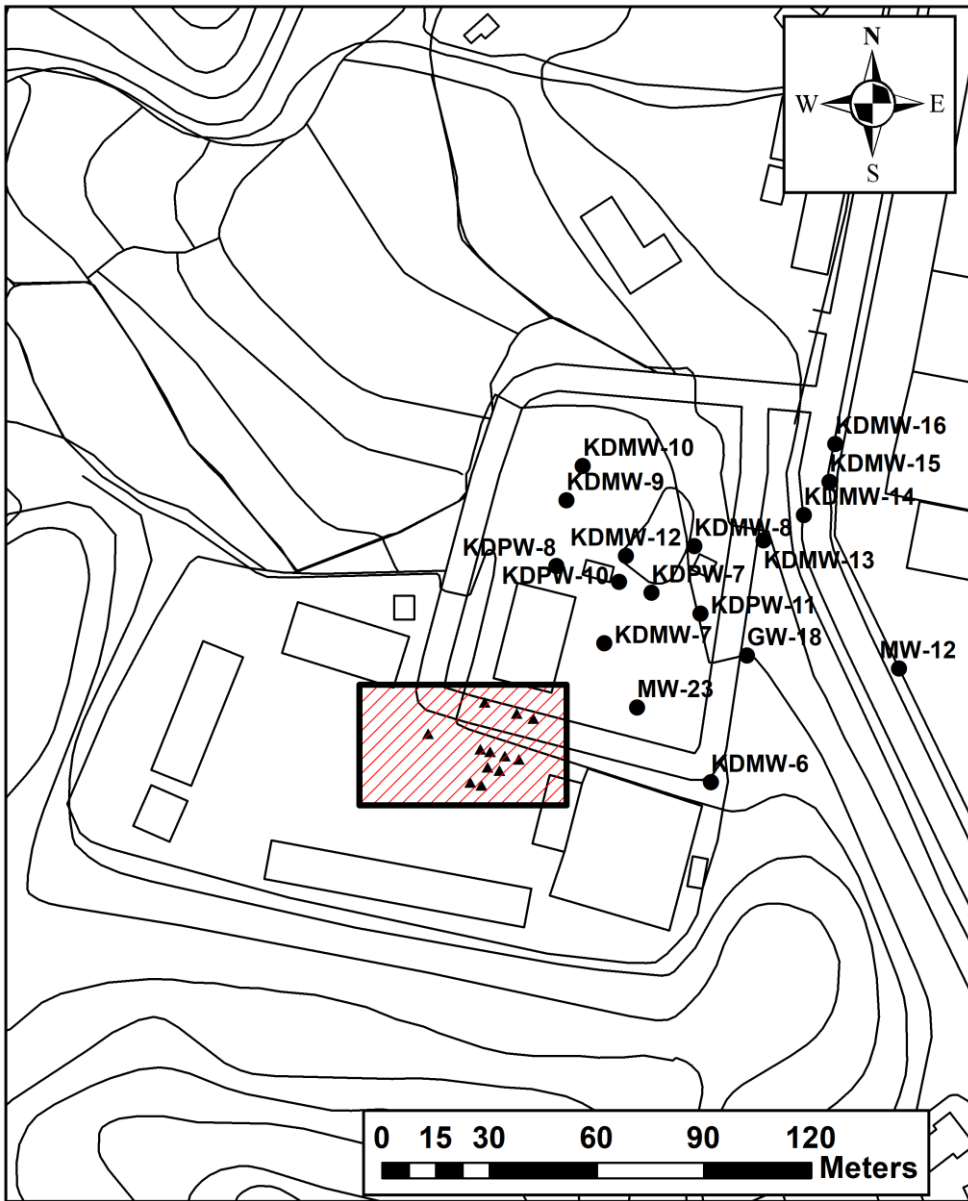


Figure 2-10. The location of wells which are applied to calculate the WCI. Red shaded box indicates hot source zone and black dots, triangular dots indicate pre-existed wells in WIC and wells located in hot source zone, respectively.

3 RESULTS AND DISCUSSION

3.1 Benchmark problem

3.1.1 Initial state of benchmark problem

Figure 3-1 presents the initial distribution of groundwater head and the concentration of TCE in a benchmark problem. The figure includes cross dots to indicate the locations of existing pumping wells, while a black square represents the source zone of TCE. The simulation time for the benchmark model is set at 1820 days. The groundwater flow simulation in the benchmark model reveals that the flow direction is from top to bottom. This flow pattern is primarily influenced by the constant head boundary at the upper and lower boundaries of the aquifer. Additionally, the presence of two pumping wells in the system affects the distribution of hydraulic head, leading to drawdown in the pumping wells. Regarding TCE transport model, the simulation assumes no degradation of TCE and considers only advection and dispersion as the TCE transport. This implies that the movement of TCE is mainly driven by the flow of groundwater and the spreading effects caused by dispersion.

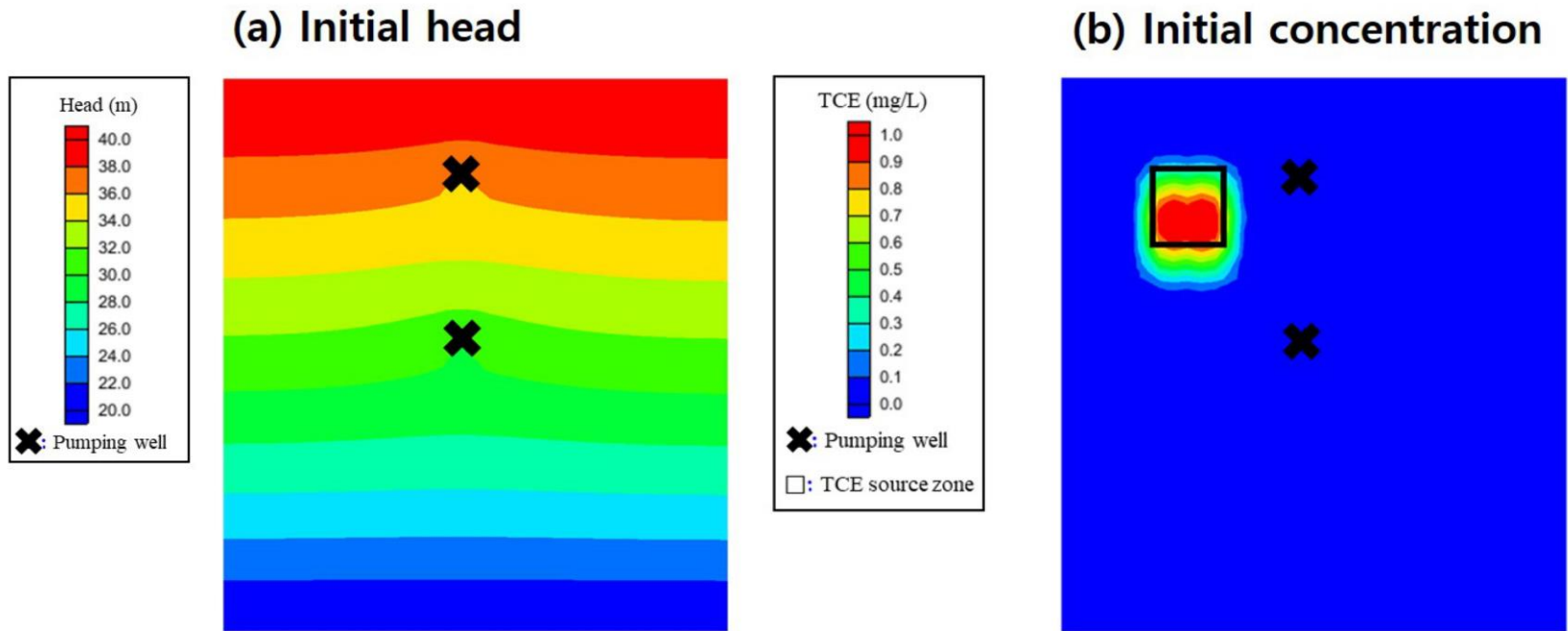


Figure 3-1. Initial distribution of (a) head and (b) TCE concentration. Cross dot indicate existing pumping well. Black box at (b) indicates TCE source zone with value of 1 mg/L.

3.1.2 Results of optimized model

Figure 3-2 illustrates the Pareto optimal front obtained through the application of NSGA-II for TCE solute transport model after 200 generations. In this multi-objective optimization problem, a set of optimal solutions is obtained that minimizes both the total mass of TCE and the associated cost, resulting in the Pareto optimal front. As the evolution progresses, the Pareto optimal front becomes more ideal, and the tradeoff between two objectives can be identified. In the figure, the green solid line represents the mean cost of all points, while the blue and red solid lines represent $\pm 30\%$ deviation from the mean cost. Three solution points, labeled as Point A, B, and C, are selected from the 200 generations to visualize the groundwater flow and TCE transport with their respective optimized pumping rates. Points A, B, and C correspond to -30%, 0%, and +30% deviation from the mean cost value.

Figure 3-3 shows the groundwater flow modeling result for Points A, B, and C. Since there is a positive correlation between cost and pumping rate, Point C exhibits a higher drawdown compared to the other two points. However, for all points, the pre-existing pumping well does not induce significant drawdown at their respective locations.

Figure 3-4 presents the TCE transport modeling results for each optimal solution. As Point C has a higher pumping rate in the additional pumping well, the concentration of TCE is lower in the center of the plume, and the plume itself becomes smaller compared to other solutions. However, Points A and B show less reduction in concentration compared to Point C. Table 3-1 provides the locations of wells for each solution depicted in Figure 3-4. The pumping rate for the two pre-existing pumping wells (EP) located outside the hot source zone is reduced, while the pumping rate for the additional pumping well (AP) that is located in the hot source zone increases, resulting in a decrease in the total mass of TCE. These results demonstrate that NSGA-II performs well in addressing the multi-objective optimization problem

associated with groundwater remediation, considering the conflicting objectives involved.

Pareto optimal front

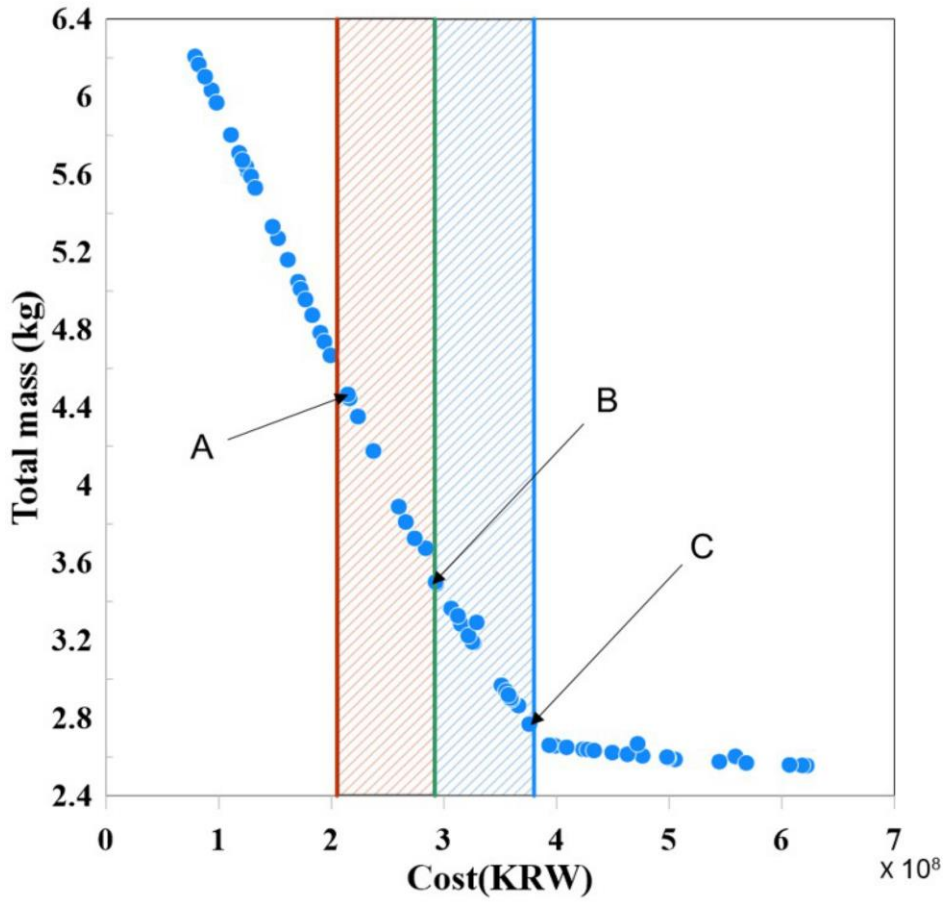


Figure 3-2. Pareto optimal front of NSGA-II at final generation with value of 100. Green solid line indicates the mean cost of all points. Blue and red line are set to $\pm 30\%$ boundaries of average cost, respectively. Point A, B, and C indicate optimal solutions at -30% , mean, and $+30\%$ costs.

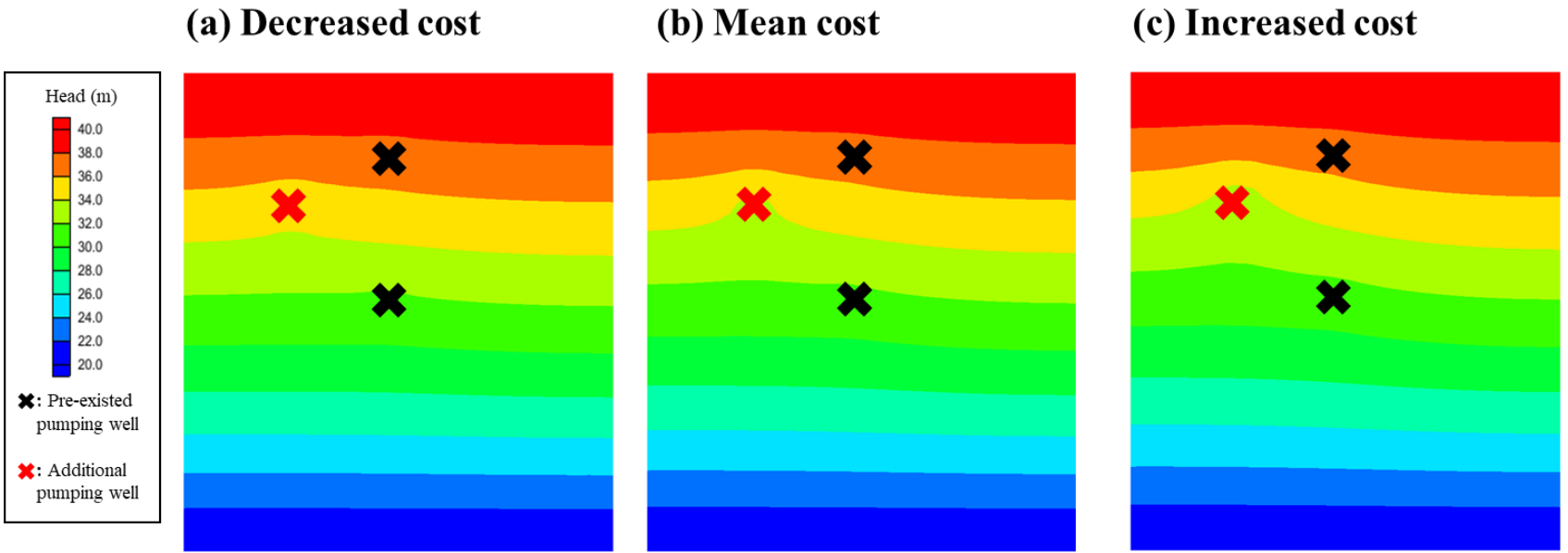


Figure 3-3. Best results of NSGA-II subject to (a) decreased cost (b) mean cost (c) increased cost; Head distribution. Black cross dots denote pre-existing pumping well and red cross dot indicates additional pumping well installs after optimization.

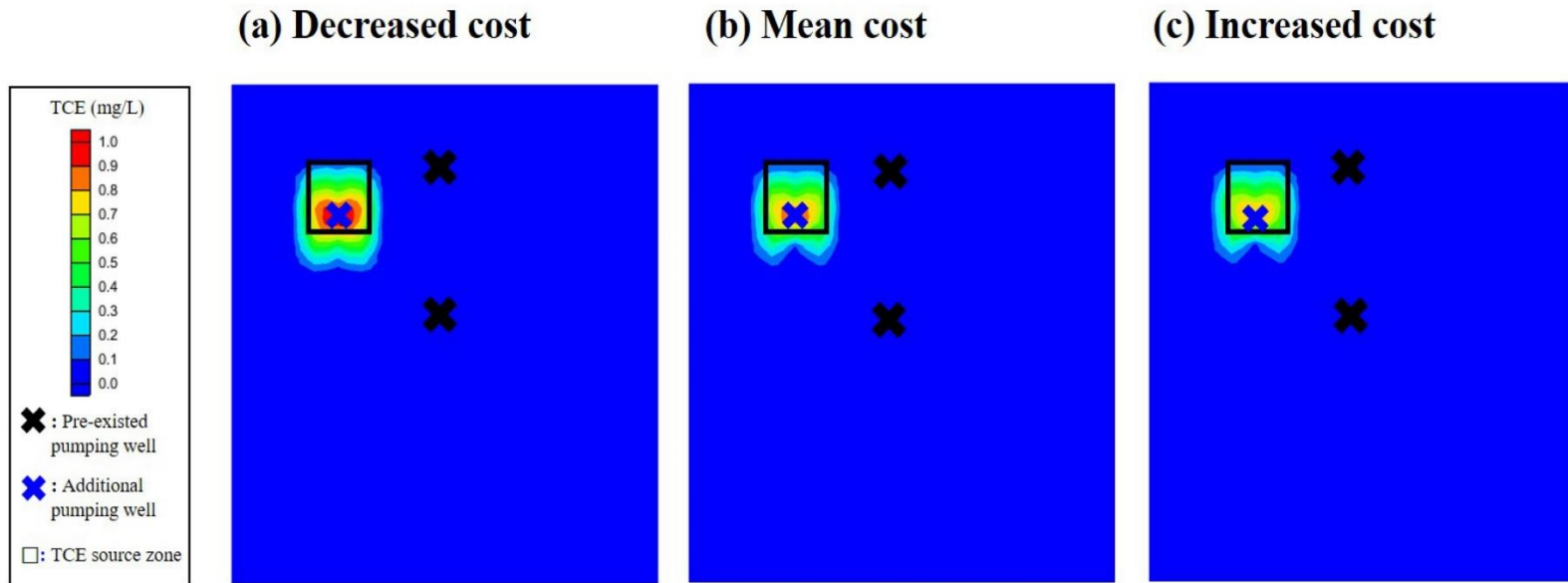


Figure 3-4. Best results of NSGA-II subject to (a) decreased cost (b) mean cost (c) increased cost; TCE concentration distribution. Black cross dots denote pre-existing pumping well, blue cross dot indicates additional pumping well installs after optimization and black box indicates TCE source zone.

Table 3-1. Optimal pumping well locations and pumping rate for solutions selected in Figure 3-2. EP and AP are pumping rate for pre-existed, and additional pumping well, respectively.

Coordinate System: Cartesian coordinate system

Point	Additional well location		EP_1 (m ³ /day)	EP_2 (m ³ /day)	AP (m ³ /day)	Cost (10 ⁸ KRW)	Total mass (kg)
	X	Y					
A	1125.0	3625.0	250	250	827	2.07	4.56
B	1125.0	3625.0	258	252	1396	2.97	3.47
C	1125.0	3625.0	250	250	1981	3.87	2.68

3.1.3 Relative performance assessment

Figure 3-5 provides a comparison of the performance between the Genetic Algorithm (GA) and NSGA-II. The results obtained from GA, denoted as Solution X, Y, Z, and W in Figure 3-5, are achieved by adjusting the weight for a single objective function that combines the pumping cost and total mass term. These GA results are found to be close to the Pareto optimal front obtained by NSGA-II, indicating their EF in approximating the optimal solutions. According to Wang and Zheng (1999), it has been established that the convergence of GA to the global optimal solution can be ensured by using an adequate number of generations and populations. The results in Figure 3-6 show the plot of the objective function value with respect to the generation number demonstrates convergence after 80 generations. Considering that the global optimal solution obtained by GA closely align with the Pareto optimal front obtained by NSGA-II, both GA and NSGA-II exhibit EF for the given optimization problem. Based on these results, it can be concluded that the NSGA-II algorithm has shown applicability to optimization problems related to pump-and-treat.

Comparison of NSGA-ii and GA

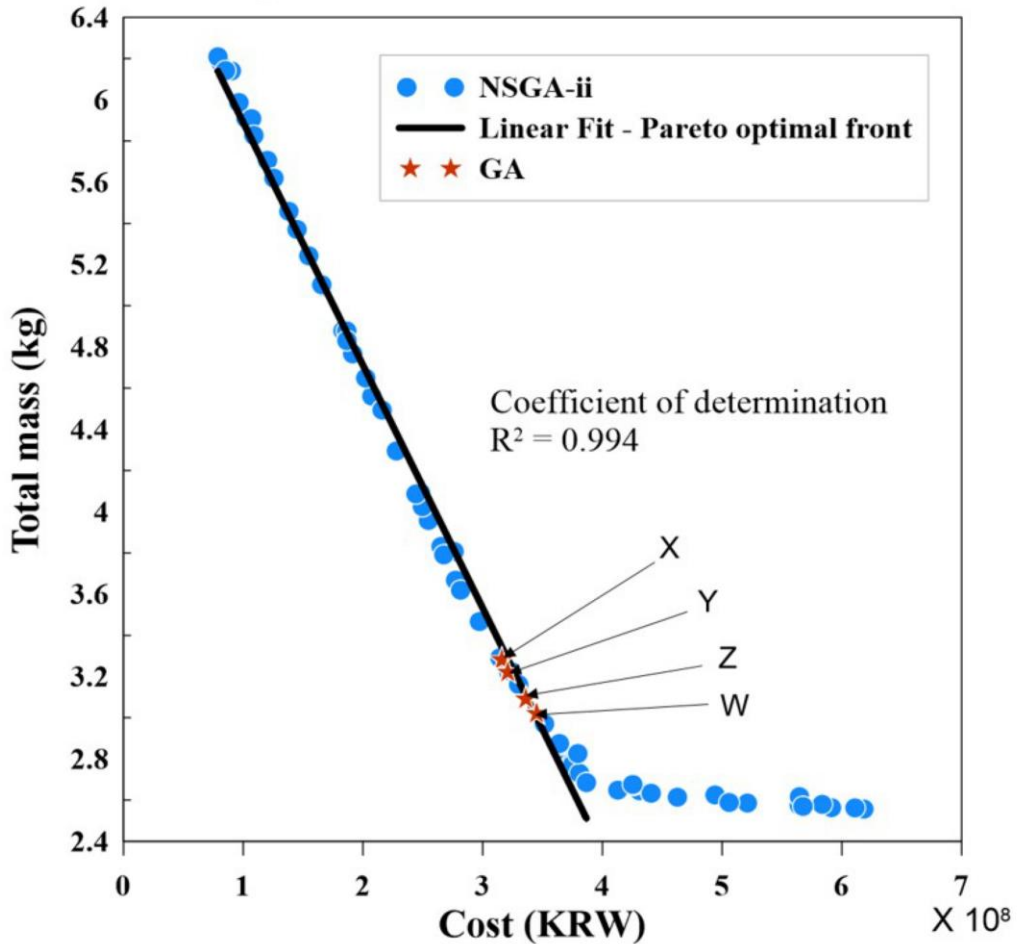


Figure 3-5. Comparison of solutions using GA and NSGA-II. Blue dots indicate optimal solution sets obtained by NSGA-II and red star indicates optimal solution obtained by GA. Black solid line indicates the linear fit line for the Pareto optimal front.

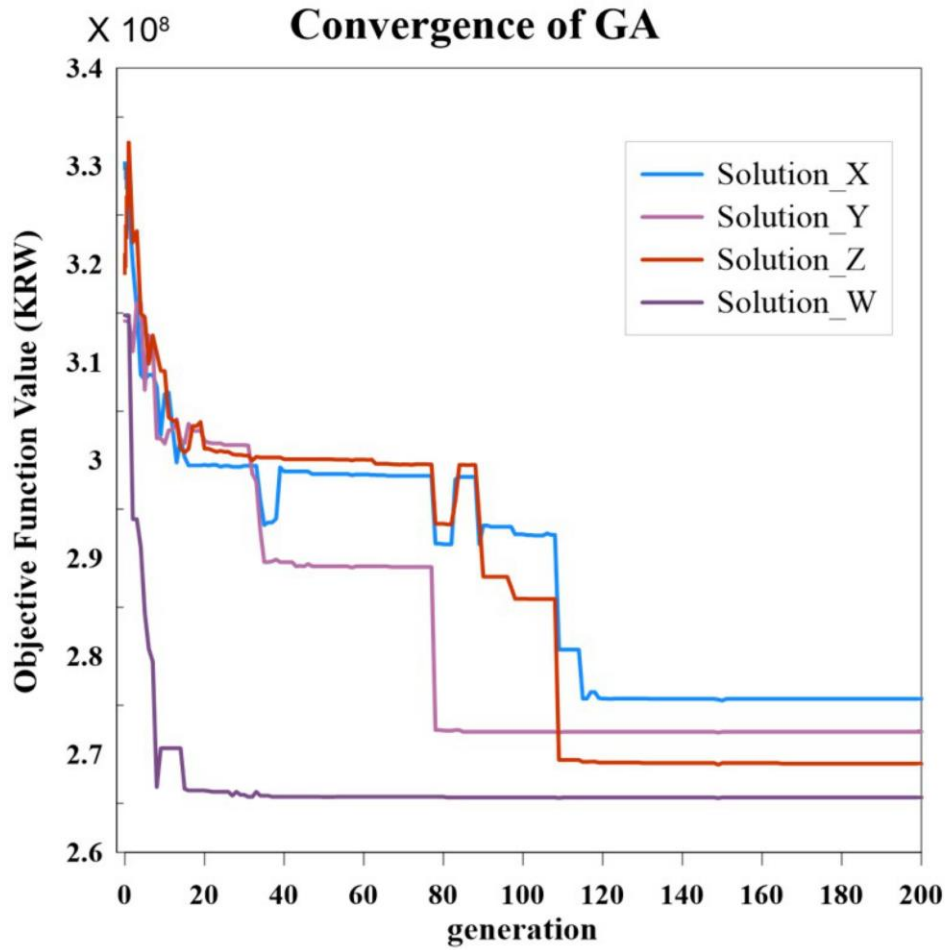


Figure 3-6. Plot of objective function value versus generation number for each optimal solution obtained by GA.

3.2 Regional scale model

3.2.1 Distribution of hydrogeological and initial concentration

Figure 3-7 displays the distribution of hydraulic conductivity field at the alluvial layer using the kriging method. With the exception of specific well regions such as SKW-7 or KDMW-8, the estimated hydraulic conductivity near the RAO exhibits low values compared to other parts of the model. According to Park et al. (2011), the hydraulic conductivity near the Wonju stream displays high values, and the kriging method effectively illustrates the distribution of hydraulic conductivity in this area.

In this study, the IDW method is employed to estimate the concentration distribution of TCE, as depicted in Figure 3-8. The region near the RAO displays a higher concentration of TCE, compared to other areas. Previous studies indicate that the RAO serves as the hot source zone for TCE, and the IDW method effectively captures the initial concentration distribution of TCE in this area (Yang et al. 2012; Lee et al. 2013).

Coordinate system: EPSG 5186

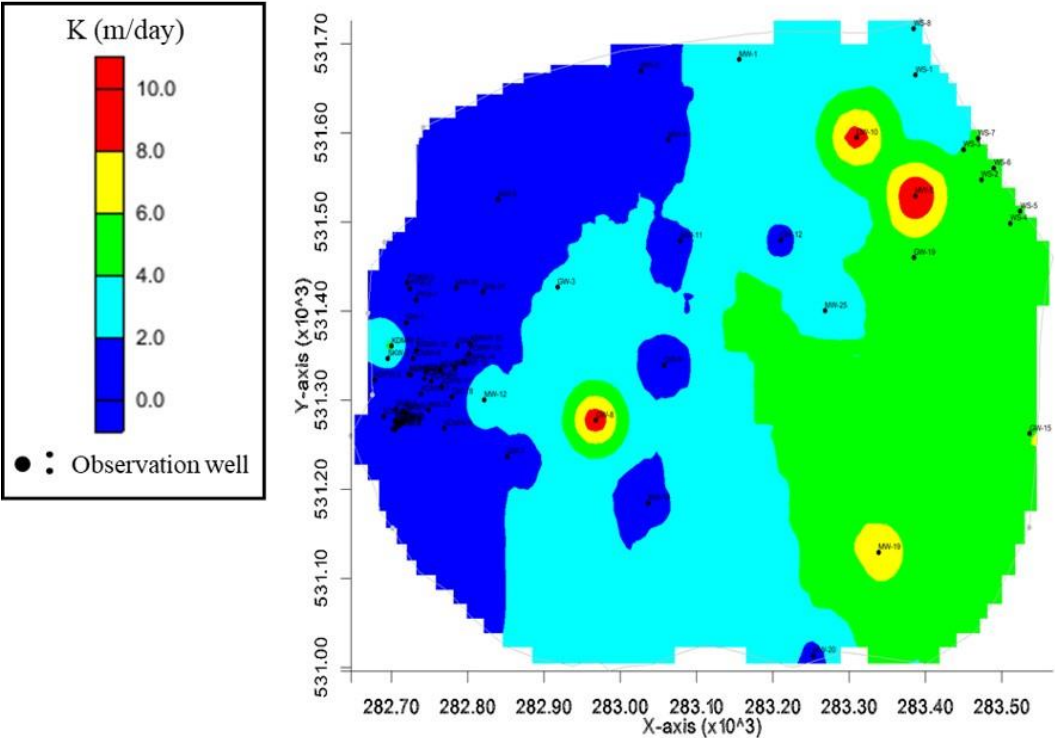


Figure 3-7. Distribution of hydraulic conductivity at alluvial aquifer of WIC site.

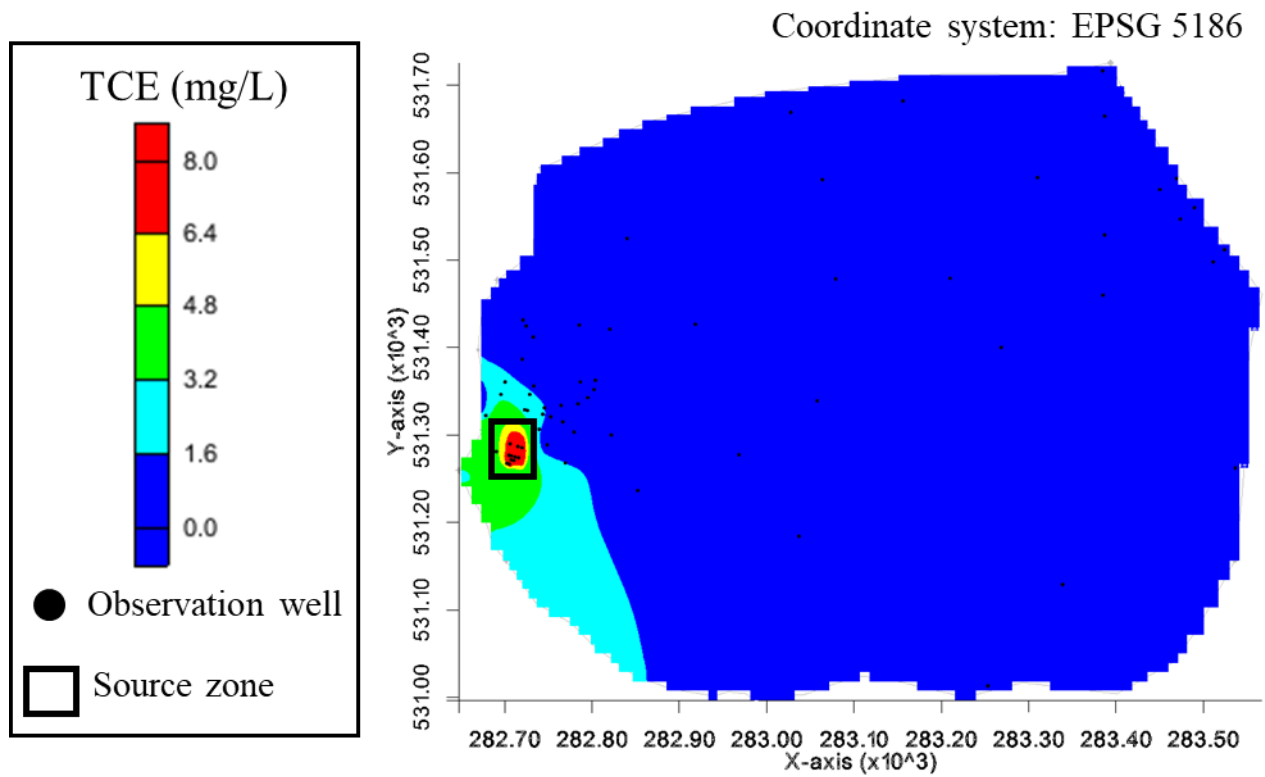


Figure 3-8. Initial concentration distribution of TCE in WIC. Black dots indicate observation well and black box indicate source zone of TCE.

3.2.2 Calibration of regional scale model

Figure 3-9 shows the initial simulation result of groundwater head and TCE transport model at the Wonju Industrial Complex (WIC). A suggestion for drinking water is that the concentration of TCE should be under 0.03 mg/L. In view of modeled initial condition, the WIC region is highly contaminated that is over 3.00 mg/L of TCE concentration at the alluvial aquifer.

A notable change in hydraulic head is observed near the RAO, whereas the changes in hydraulic head are less prominent towards the Wonju stream. The simulation result showed that the predominant direction of groundwater flow is from the RAO towards the Wonju stream.

The initial calculated head with a steady state is compared to the observed head as shown in Figure 3-10a. To evaluate the performance of the steady-state model, two metrics, namely the Root Mean Square Error (RMSE) and Mean Absolute Error (MAE), are used. The RMSE represents the average magnitude of the residuals between the observed and simulated hydraulic heads. On the other hand, the MAE quantifies the average absolute difference between the observed and simulated hydraulic heads. The RMSE and MAE are 3.10 m and 1.97 m, respectively. These metrics collectively indicate that the steady-state flow model performs well in capturing the dynamics of the system and provides a reasonable representation of the observed data.

After initialization of groundwater head and concentration, transient simulation is performed to identify that the current status of the regional scale model is a good agreement with time series groundwater and concentration at hot source zone, where the higher concentration is observed, compared to other regions (Figure 3-10b, c). In the groundwater flow model, the groundwater head varies in response to rainfall events. Although the concentration of TCE gradually decreases over time, there is a seasonal

fluctuation in concentration during rainfall events. This fluctuation is attributed to the dissolution of TCE that is trapped in the vadose zone.

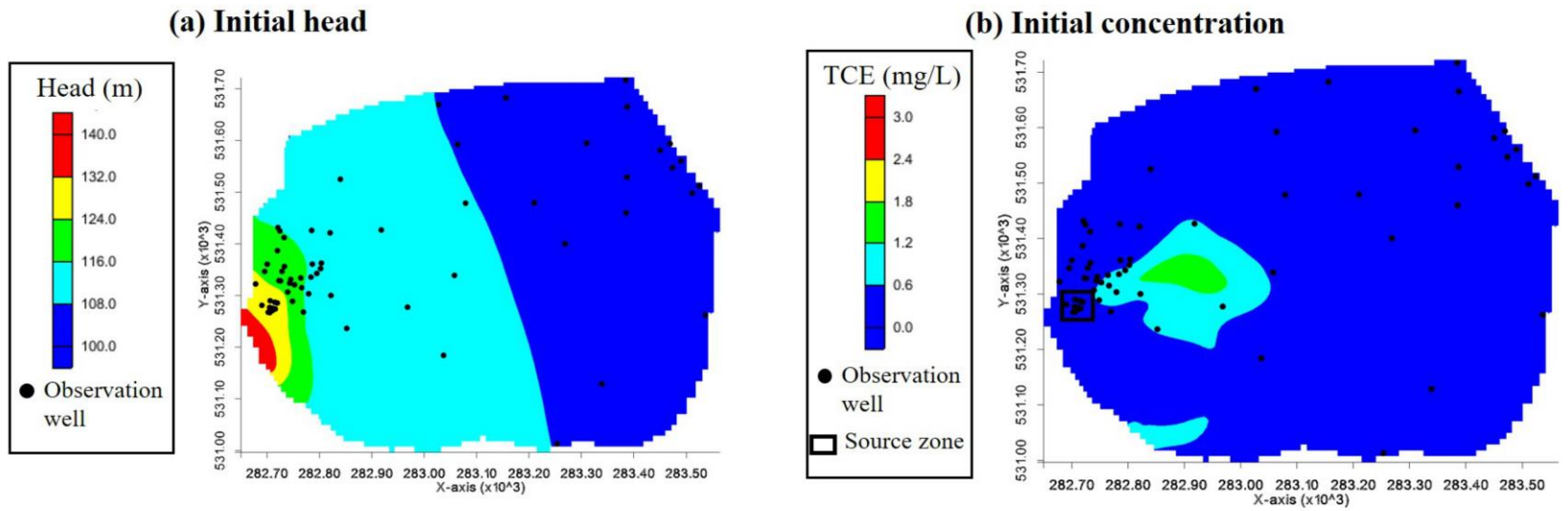


Figure 3-9. (a) Modeled head distribution of steady state flow. (b) modeled TCE concentration distribution with MT3D model. Black dots indicate observation wells and black box indicates TCE source zone.

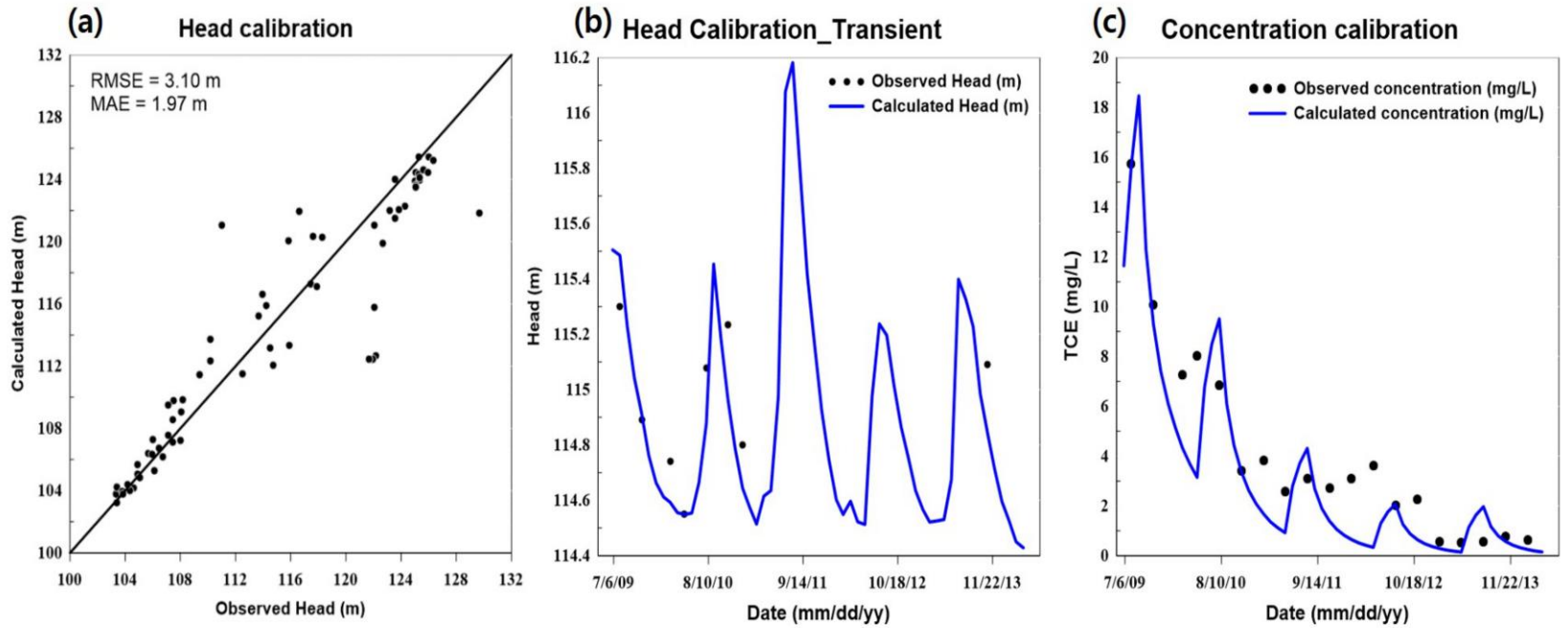


Figure 3-10. (a) Comparison between modeled and observed head with steady state groundwater flow. (b,c) Time series modeled and observed of head at GW-17 and concentration at KDPW-2 where located at hot source zone.

3.2.3 Optimization in pump-and-treat operation

The optimal solution set for the pump-and-treat operation with the two different scenarios is shown in Figure 3-11. It displays the trade-off relationship between cost and concentration, indicating the challenges in achieving an ideal trade-off. The complexity of input terms, particularly the reactive term of the solute, contributes to a non-ideal trade-off relationship.

Comparing the optimal solution sets of the different remediation scenarios, the pump-and-treat operation under the rainy season exhibits a significant reduction in concentration compared to continuous operation (Figure 3-11). However, when considering a low remediation cost, which implies a low pumping rate, both scenarios show a similar reduction in total concentration.

To evaluate the performance of the pump-and-treat operation, the optimized pumping rate for both scenarios at maximum cost in each remediation scenario is assigned to the initial groundwater flow model for 1740 days (Figure 3-12). The total pumping rate is 505 m³/day for continuous operation and 387 m³/day for rainy season operation. The transient simulation with the optimized pumping rate displays a reduction in the size of the contaminant plume and a decrease in concentration. Rainy season operation shows a greater reduction in both size of the contaminant plume and the maximum concentration at the hot source zone.

Figure 3-13 illustrates the total mass for each scenario. The base model without any pumping displays a continuous reduction in the total TCE concentration due to natural degradation factors. The rainy season operation shows a greater reduction in the total concentration. This is due to the fact that pumping during the rainy season could remove not only the pre-existing dissolved phase of TCE but also the trapped TCE that has come into contact with water table. Although the continuous operation does not display a significant reduction in the total mass before 1300 days, both scenarios

exhibit a similar total mass at the final simulation time. This is because the pump-and-treat operation is only conducted near the hot source zone and local source zone, which are not included in the observation wells.

Based on these findings, it is evident that operating the pump-and-treat system specifically during the rainy season can yield great remediation performance compared to continuous operation in this study site. Especially, this operation system would be applicable at the contaminated site where trapped contaminants exist in the vadose zone. Additionally, accounting for the uncertain variation of TCE with respect to the water table is important when determining optimal pump-and-treat strategies.

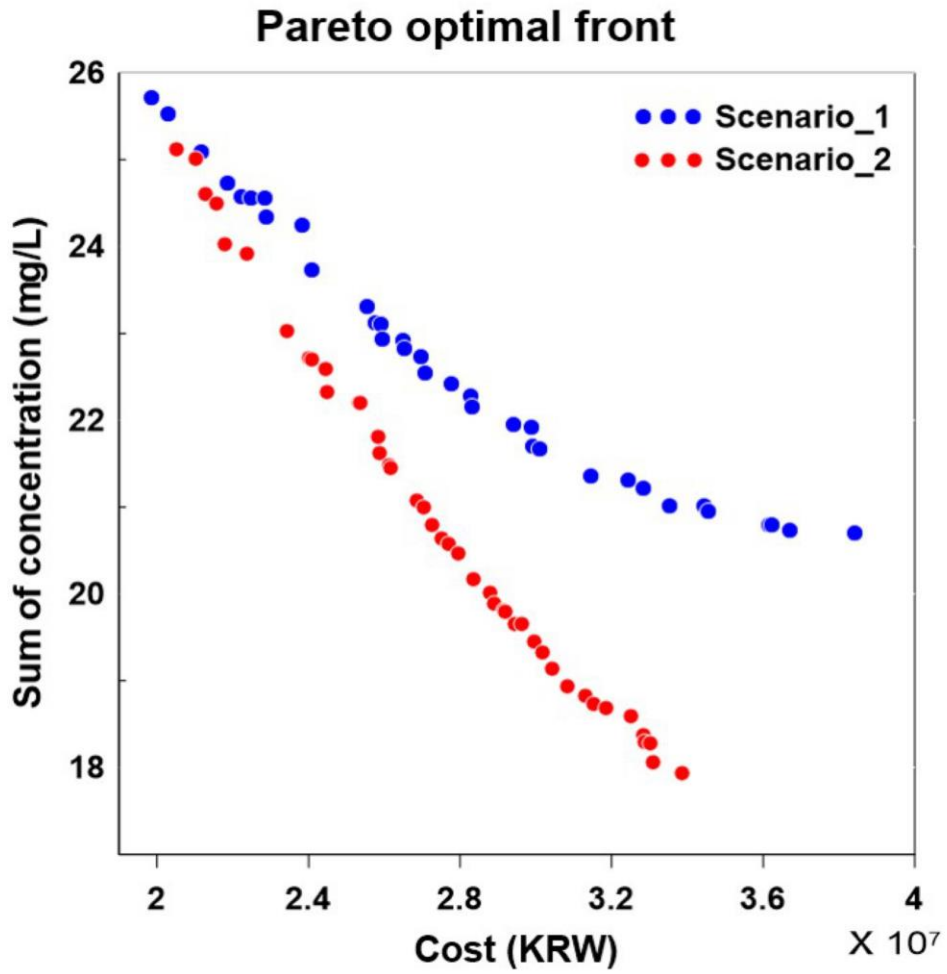


Figure 3-11. Pareto optimal front in final generation. Blue and red dot indicate the different remediation scenarios.

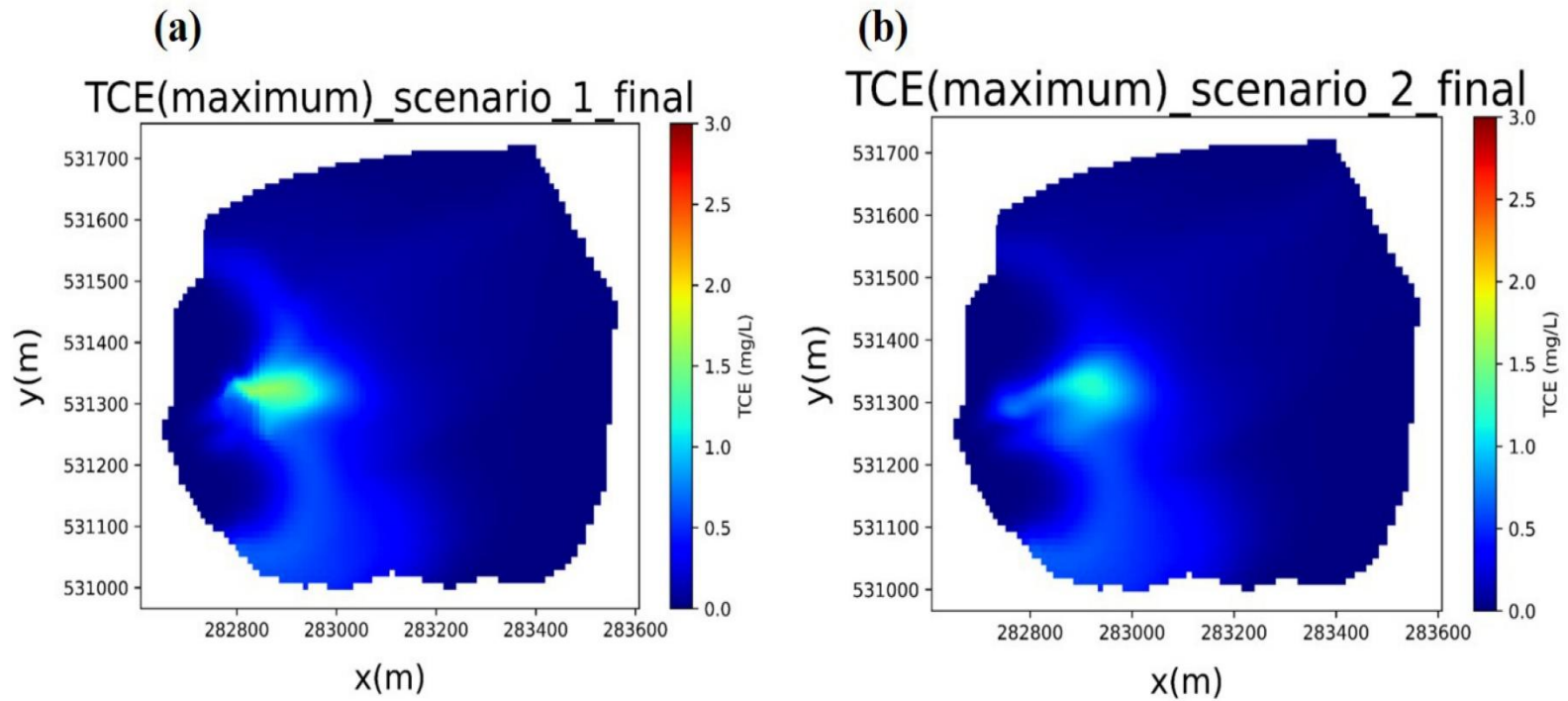


Figure 3-12. Optimized simulation result at final time that is related to (a) first pump-and-treat scenario with the greatest decreasing of TCE (b) second pump-and-treat scenario with the greatest decreasing of TCE.

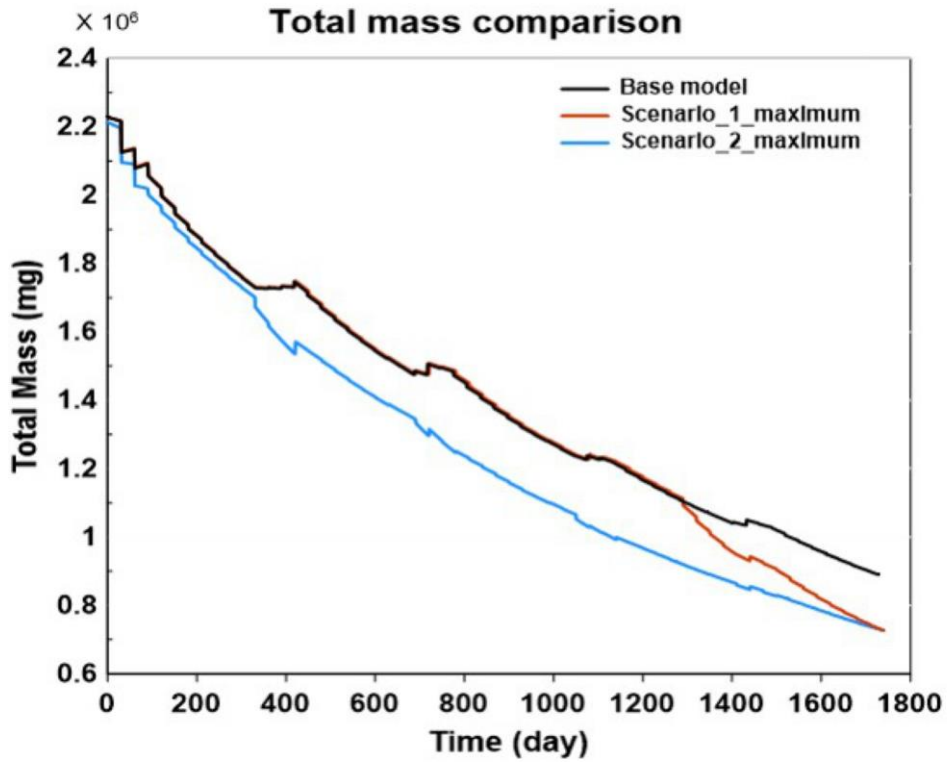


Figure 3-13. Total mass change of TCE depending on maximum cost in pump-and-treat scenarios. The black line indicates the total concentration change of the base model without pumping. The red and blue lines represent continuous and rainy season operation scenarios, respectively.

3.2.4 Well Contribution Index at alluvial aquifer

The analysis of the Well Contribution Index (WCI) is performed to obtain the optimal solutions for different cost scenarios. The optimal solution for the minimum cost and median cost is used to calculate the WCI. However, when the optimal solution for the maximum cost is applied, the pumping rates reach their maximum values, making it difficult to identify which wells significantly contribute to groundwater remediation, as all wells are operating at their maximum pumping rate. By considering only the pumping rate, different wells show significant contributions in the two remediation scenarios. First scenario assumed continuous operation, while second scenario assumed operating only at the rainy season. In the first scenario, wells GW-7, GW-8, and KDMW-13 have notable contributions, while in the second scenario, wells MW-12, GW-18, and MW-23 contribute more to the pump-and-treat system. Wells that exhibit notable contribution in the second remediation scenario are closer to the hot source zone compared to those in the first remediation scenario. This can be attributed to the fact that the pump-and-treat was implemented during the initial stage. Also during the pump-and-treat, trapped TCE in the vadose zone is removed before it disperses. The locations of these wells can be observed in Figure 3-14.

To calculate the WCI, well specification data such as the length of the screen is taken into account. The results of the WCI analysis can be found in Table 3-2 and Table 3-3. These tables show that, compared to considering only the pumping rate, different wells exhibit significant contributions in each scenario. In the first scenario, wells KDMW-13, KDMW-6 and GW-7 are prominent contributors, while in the second scenario, wells KDPW-7, KDMW-8, and KDPW-11 have higher contributions. Notably, well KDPW-7, located near the hot source zone, demonstrates better performance in the pump-and-treat based on long-term monitoring and pilot-test results related to remediation in the Wonju Industrial Complex (Jeon et al. 2013; Lee et al.

2013). Overall, the proposed Well Contribution Index (WCI) provides valuable insights into prioritizing wells for optimal pump-and-treat operations in contaminated alluvial aquifers. By considering simulation results and site characteristics, the WCI can help find the most effective wells for groundwater remediation efforts.

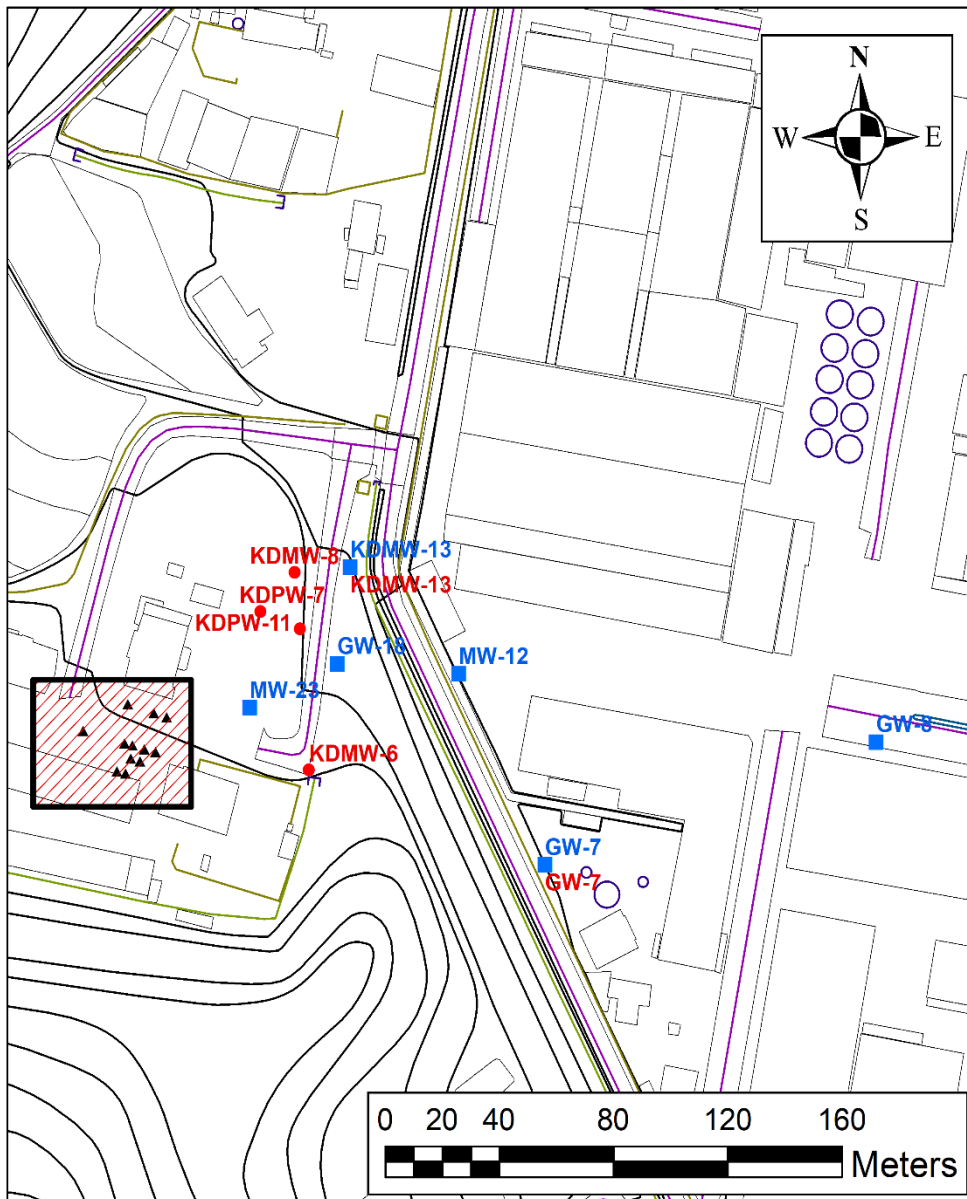


Figure 3-14. Location of wells which contribute much to pump-and-treat subject to several scenarios. Blue labeled points, red labeled points, triangular point indicate contribute much for pump-and-treat only considered pumping rate, considered both specification of well and pumping rate, and well located in hot source zone, respectively.

Table 3-2. Calculation of the WCI for continuous operation.

Well	WCI_p	WCI_s	WCI_{de}	WCI_{di}	Overall
KDMW-13	16	17.5	17	10	15.95
KDMW-6	14.5	10	9.5	14.5	12.65
GW-7	17.5	7	9.5	5	12.3
KDPW-10	6	17.5	17	14.5	11.4
GW-18	17.5	4.5	5	5	11.1
KDPW-7	6	16	17	14.5	10.95
KDPW-8	6	15	15	14.5	10.45
KDMW-8	6	13.5	14	14.5	9.9
KDPW-11	12	9	7	5	9.9
KDMW-9	6	11.5	12	14.5	9.1
KDMW-12	6	13.5	12	5	8.75
MW-12	14.5	1	1	5	8.15
KDMW-14	13	2	2	5	7.8
KDMW-15	11	4.5	3.5	5	7.7
KDMW-7	6	8	8	14.5	7.65
KDMW-10	1	11.5	12	14.5	6.6
MW-23	6	4.5	6	5	5.45
KDMW-16	6	4.5	3.5	5	5.2

Table 3-3. Calculation of the WCI for optimal pumping rate of rainy season operation.

Well	WCI_p	WCI_s	WCI_{de}	WCI_{di}	Overall
KDPW-7	13	16	17	14.5	14.45
KDMW-8	11	13.5	14	14.5	12.4
KDPW-11	16	9	7	5	11.9
KDMW-7	14	8	8	14.5	11.65
KDMW-6	12	10	9.5	14.5	11.4
GW-18	17.5	4.5	5	5	11.1
KDMW-13	6	17.5	17	10	10.95
KDPW-8	6	15	15	14.5	10.45
MW-23	15	4.5	6	5	9.95
MW-12	17.5	1	1	5	9.65
KDMW-9	6	11.5	12	14.5	9.1
KDMW-10	6	11.5	12	14.5	9.1
KDPW-10	1	17.5	17	14.5	8.9
KDMW-12	6	13.5	12	5	8.75
GW-7	6	7	9.5	5	6.55
KDMW-15	6	4.5	3.5	5	5.2
KDMW-16	6	4.5	3.5	5	5.2
KDMW-14	6	2	2	5	4.3

4 CONCLUSION

Simulation-Optimization modeling, coupling MODFLOW and MT3D with NSGA-II, was used to suggest an optimal groundwater remediation plan for the benchmark problem and a real contamination site such as the Wonju Industrial Complex (WIC). First, the performance of NSGA-II was evaluated in the benchmark problem by applying two metrics; Effectiveness (EF) and Efficiency (EY) which evaluate algorithm convergence and improvement of computation cost. After confirming the application of NSGA-II in the benchmark problem, the Well Contribution Index (WCI) was proposed for two remediation scenarios in WIC.

The results from the benchmark problem showed that NSGA-II performed well for conflicting objectives, such as cost and remaining contaminations. Furthermore, those showed that a good EF indicates the attainment of global optimal solution and good EY which means reducing computation cost. Based on the relative performance assessment, NSGA-II algorithm shows an improvement in computation cost with obtaining the global optimal solution and it indicates the applicability of the algorithm to the optimal operation of pump-and-treat.

For the alluvial aquifer model, operating pump-and-treat only during the rainy season proved to reduce the concentration of TCE and effectively prevent plume migration in this study site. This result indicates that operating only during the rainy season could additionally extract trapped TCE in the vadose zone because the rising of the water table by rainfall leads to the contacting of the trapped TCE. Moreover, the results of WCI considering the well data and differences of pumping rate showed that KDPW-7 which is located near the hot source zone along the groundwater flow direction can be contributed significantly to the pump-and-treat operation. Previous pilot tests of pump-and-treat performed at KDPW-7 have shown good performance of

the operation, indicating that the WCI proposed in this study could be used to prioritize the selection of pumping wells in real pump-and-treat operations.

Overall, results obtained from this study can be utilized to derive effective pump-and-treat strategies not only in general DNAPL contaminated site and site-specific condition where contaminants trapped in the vadose zone have existed but also support the optimal decision-making for groundwater remediation.

5 REFERENCE

- Ahlfeld DP, Mulvey JM, Pinder GF (1988) Contaminated groundwater remediation design using simulation, optimization, and sensitivity theory: 2. Analysis of a field site. *Water Resour Res* 24:443–452. <https://doi.org/10.1029/WR024i003p00443>
- Aly AH, Peralta RC (1999) Comparison of a genetic algorithm and mathematical programming to the design of groundwater cleanup systems. *Water Resour Res* 35:2415–2425. <https://doi.org/10.1029/1998WR900128>
- Asghar E, Baqai AA, Khaleeq uz Zaman U (2015) Performance of NSGA-II and WGA in Macro Level Process Planning considering Reconfigurable Manufacturing System. *Int Conf Flex Autom Intell Manuf* 2:320–327
- Baek W, Lee JY (2011) Source apportionment of trichloroethylene in groundwater of the industrial complex in Wonju, Korea: A 15-year dispute and perspective. *Water Environ J* 25:336–344. <https://doi.org/10.1111/j.1747-6593.2010.00226.x>
- Beheshti Z, Shamsuddin SMH (2013) A Review of Population-based Meta-Heuristic Algorithm. *Int J Adv Soft Comput its Appl* 5:1–35
- Bertsekas DP (2009) *Convex optimization theory*
- Cho I, Ju YJ, Lee SS, et al (2020) Characterization of a NAPL-contaminated site using the partitioning behavior of noble gases. *J Contam Hydrol* 235:103733. <https://doi.org/10.1016/j.jconhyd.2020.103733>
- Choe J (2013) *Geostatistics*, Sigmaphress, Seoul, Korea
- D'Ambrosio C, Lodi A, Wiese S, Bragalli C (2015) Mathematical programming techniques in water network optimization. *Eur J Oper Res* 243:774–788. <https://doi.org/10.1016/j.ejor.2014.12.039>
- Deb K, Pratap A, Agarwal S, Meyarivan T (2002) A fast and elitist multiobjective genetic algorithm: NSGA-II. *IEEE Trans Evol Comput*

- 6:182–197. <https://doi.org/10.1109/4235.996017>
- Erickson M, Mayer A, Horn J (2002) Multi-objective optimal design of groundwater remediation systems: Application of the niched Pareto genetic algorithm (NPGA). *Adv Water Resour* 25:51–65.
[https://doi.org/10.1016/S0309-1708\(01\)00020-3](https://doi.org/10.1016/S0309-1708(01)00020-3)
- Harbaugh A (2005) MODFLOW-2005 , The U . S . Geological Survey Modular Ground-Water Model — the Ground-Water Flow Process MODFLOW-2005 , The U . S . Geological Survey Modular Ground-Water Model — the Ground-Water Flow Process. Open-File Report, US Geol Surv
- Huang C, Mayer AS (1997) Pump-and-treat optimization using well locations and pumping rates as decision variables. *Water Resour Res* 33:1001–1012. <https://doi.org/10.1029/97WR00366>
- Jackson RE (1998) The migration, dissolution, and fate of chlorinated solvents in the urbanized alluvial valleys of the southwestern USA. *Hydrogeol J* 6:144–155. <https://doi.org/10.1007/s100400050140>
- Jeon W-H, Lee J-Y, Kwon H-P, et al (2013) Evaluation of Contaminant Concentrations in Wet and Dry Seasons during Pump-and-Treat Pilot Tests. *J Soil Groundw Environ* 18:18–31.
<https://doi.org/10.7857/jsge.2013.18.6.018>
- Jeyakumar V, Rubinov AM, Wu ZY (2007) Non-convex quadratic minimization problems with quadratic constraints: Global optimality conditions. *Math Program* 110:521–541.
<https://doi.org/10.1007/s10107-006-0012-5>
- Kim H-M, Hyun Y, Lee K-K (2007) Remediation of TCE-Contaminated Groundwater in a Sandy Aquifer Using Pulsed Air Sparging: Laboratory and Numerical Studies. *J Environ Eng* 133:380–388.
[https://doi.org/10.1061/\(asce\)0733-9372\(2007\)133:4\(380\)](https://doi.org/10.1061/(asce)0733-9372(2007)133:4(380))
- Ko NY, Lee KK, Hyun Y (2005) Optimal groundwater remediation design of a pump and treat system considering clean-up time. *Geosci J* 9:23–

31. <https://doi.org/10.1007/BF02910551>
- Konak A, Coit DW, Smith AE (2006) Multi-objective optimization using genetic algorithms: A tutorial. *Reliab Eng Syst Saf* 91:992–1007.
<https://doi.org/10.1016/j.res.2005.11.018>
- Korea water resources and corporation (2011) Report of the basic investigation research of groundwater in Wonju
- Langwaldt JH, Puhakka JA (2000) On-site biological remediation of contaminated groundwater: A review. *Environ Pollut* 107:187–197.
[https://doi.org/10.1016/S0269-7491\(99\)00137-2](https://doi.org/10.1016/S0269-7491(99)00137-2)
- Lee S-S, Kim H-M, Lee SH, et al (2013) Evidences of in Situ Remediation from Long Term Monitoring Data at a TCE-contaminated Site, Wonju, Korea. *J Soil Groundw Environ* 18:8–17.
<https://doi.org/10.7857/jsge.2013.18.6.008>
- Lee YC, Kwon TS, Yang JS, Yang JW (2007) Remediation of groundwater contaminated with DNAPLs by biodegradable oil emulsion. *J Hazard Mater* 140:340–345. <https://doi.org/10.1016/j.jhazmat.2006.09.036>
- Lien PJ, Yang ZH, Chang YM, et al (2016) Enhanced bioremediation of TCE-contaminated groundwater with coexistence of fuel oil: Effectiveness and mechanism study. *Chem Eng J* 289:525–536.
<https://doi.org/10.1016/j.cej.2016.01.011>
- Maier HR, Kapelan Z, Kasprzyk J, et al (2014) Evolutionary algorithms and other metaheuristics in water resources: Current status, research challenges and future directions. *Environ Model Softw* 62:271–299.
<https://doi.org/10.1016/j.envsoft.2014.09.013>
- Mategaonkar M, Eldho TI (2012) Groundwater remediation optimization using a point collocation method and particle swarm optimization. *Environ Model Softw* 32:37–48.
<https://doi.org/10.1016/j.envsoft.2012.01.003>
- McKinney DC, Lin M -D (1994) Genetic algorithm solution of groundwater management models. *Water Resour Res* 30:1897–1906.

<https://doi.org/10.1029/94WR00554>

- Mirzaee M, Safavi HR, Taheriyoun M, Rezaei F (2021) Multi-objective optimization for optimal extraction of groundwater from a nitrate-contaminated aquifer considering economic-environmental issues: A case study. *J Contam Hydrol* 241:103806.
<https://doi.org/10.1016/j.jconhyd.2021.103806>
- Mondal A, Eldho TI, Rao VVSG (2010) Multiobjective Groundwater Remediation System Design Using Coupled Finite-Element Model and Nondominated Sorting Genetic Algorithm II. *J Hydrol Eng* 15:350–359. [https://doi.org/10.1061/\(asce\)he.1943-5584.0000198](https://doi.org/10.1061/(asce)he.1943-5584.0000198)
- Moon J-W, Moon H-S, Kim H, Roh Y (2005) Remediation of TCE-contaminated groundwater using zero valent iron and direct current: experimental results and electron competition model. *Environ Geol* 48:805–817. <https://doi.org/10.1007/s00254-005-0023-1>
- Park DK, Ko NY, Lee KK (2007) Optimal groundwater remediation design considering effects of natural attenuation processes: Pumping strategy with enhanced-natural-attenuation. *Geosci J* 11:377–385.
<https://doi.org/10.1007/BF02857053>
- Park YC, Jeong JM, Eom S Il, Jeong UP (2011) Optimal management design of a pump and treat system at the industrial complex in Wonju, Korea. *Geosci J* 15:207–223. <https://doi.org/10.1007/s12303-011-0018-8>
- Peralta RC (2012) Multiobjective Optimization Approaches. *Groundw Optim Handb* 190–215. <https://doi.org/10.1201/b11866-13>
- Reddy K (2008) Physical and chemical groundwater remediation technologies. In: Darnault CJG (ed) *Overexploitation and contamination of shared groundwater resources*. Springer 257–274
- Rivett MO, Chapman SW, Allen-King RM, et al (2006) Pump-and-treat remediation of chlorinated solvent contamination at a controlled field-experiment site. *Environ Sci Technol* 40:6770–6781.

<https://doi.org/10.1021/es0602748>

- Rivett MO, Feenstra S, Cherry JA (2001) A controlled field experiment on groundwater contamination by a multicomponent DNAPL: Creation of the emplaced-source and overview of dissolved plume development. *J Contam Hydrol* 49:111–149. [https://doi.org/10.1016/S0169-7722\(00\)00191-1](https://doi.org/10.1016/S0169-7722(00)00191-1)
- Sawyer CS, Ahlfeld DP, King AJ (1995) Groundwater Remediation Design Using a Three-Dimensional Simulation Model and Mixed-Integer Programming. *Water Resour Res* 31:1373–1385. <https://doi.org/10.1029/94WR02740>
- Silveira CLB, Tabares A, Faria LT, Franco JF (2021) Mathematical optimization versus Metaheuristic techniques: A performance comparison for reconfiguration of distribution systems. *Electr Power Syst Res* 196:. <https://doi.org/10.1016/j.epsr.2021.107272>
- Singh TS, Chakrabarty D (2010) Multi-objective optimization for optimal groundwater remediation design and management systems. *Geosci J* 14:87–97. <https://doi.org/10.1007/s12303-010-0010-8>
- Tabari MMR, Abyar M (2022) Development a Novel Integrated Distributed Multi-objective Simulation-optimization Model for Coastal Aquifers Management Using NSGA-II and GMS Models. *Water Resour Manag* 36:75–102. <https://doi.org/10.1007/s11269-021-03012-0>
- Teramoto EH, Pede MAZ, Chang HK (2020) Impact of water table fluctuations on the seasonal effectiveness of the pump-and-treat remediation in wet–dry tropical regions. *Environ Earth Sci* 79:1–15. <https://doi.org/10.1007/s12665-020-09182-1>
- Wang M, Zheng C (1999) Groundwater management optimization using genetic algorithms and simulated annealing: Formulation and comparison. *J Am water resources Assoc* 34:519–530
- Wang S, Mulligan CN (2006) Natural attenuation processes for remediation of arsenic contaminated soils and groundwater. *J Hazard Mater*

- 138:459–470. <https://doi.org/10.1016/j.jhazmat.2006.09.048>
- Yang JH, Lee KK (2012) Locating plume sources of multiple chlorinated contaminants in groundwater by analyzing seasonal hydrological responses in an industrial complex, Wonju, Korea. *Geosci J* 16:301–311. <https://doi.org/10.1007/s12303-012-0028-1>
- Yang JH, Lee KK, Clement TP (2012) Impact of seasonal variations in hydrological stresses and spatial variations in geologic conditions on a TCE plume at an industrial complex in Wonju, Korea. *Hydrol Process* 26:317–325. <https://doi.org/10.1002/hyp.8236>
- Yang Y, Wu J, Luo Q, Wu J (2022) An effective multi-objective optimization approach for groundwater remediation considering the coexisting uncertainties of aquifer parameters. *J Hydrol* 609:127677. <https://doi.org/10.1016/j.jhydrol.2022.127677>
- Yusoff Y, Ngadiman MS, Zain AM (2011) Overview of NSGA-II for optimizing machining process parameters. *Procedia Eng* 15:3978–3983. <https://doi.org/10.1016/j.proeng.2011.08.745>
- Zeynali MJ, Pourreza-Bilondi M, Akbarpour A, et al (2022) Optimizing pump-and-treat method by considering important remediation objectives. *Appl Water Sci* 12:1–18. <https://doi.org/10.1007/s13201-022-01785-2>
- Zheng C, Wang PP (1999) MT3DMS - A Modular Three-Dimensional Multispecies Transport Model. *Strateg Environ Res Dev Progr* 1–40

국문 초록

지하수를 수자원으로서 그 가치를 유지하기 위한 오염 정화는 필수이다. 특히, 트리클로로에틸렌 (TCE) 오염 정화 시에는 양수-처리 기술이 많이 활용되는데, 이 기술에 대해서는 비용 및 시간 효과적인 정화 설계안을 제안하는 것이 필요하다. 이를 위해, 유전 알고리즘 (GA) 라는 최적화 알고리즘을 많이 활용했지만, 다목적 최적화 문제를 다루는 데 있어 한계점이 존재하고 있다. 기존 GA의 한계점을 극복하고자 Non-dominated Sorting Genetic Algorithm-II (NSGA-II) 라는 다목적 최적화 문제를 다루는 알고리즘이 대안으로 활용되고 있다. 본 연구에서는 NSGA-II 알고리즘의 상대적인 수행 능력을 검증해보고, 충적 대수층이 TCE로 오염된 원주 우산공단 지역에서 최적의 지하수 정화 설계안을 제안하고자 한다. MODFLOW와 MT3D를 활용하여 가상의 대수층 모델과 충적 대수층 모델에서의 지하수 유동과 TCE 운송을 모의하였다. 추가적으로, 지구통계 모델을 활용하여 이질적인 수리전도도 분포와 초기 농도 분포를 구하였다. 가상의 대수층 모델에서는 NSGA-II의 상대적인 수행능력을 검증하기 위해 가중치를 포함한 유전알고리즘과 NSGA-II를 다목적 최적화 문제에 적용해 보았다. 충적 대수층 모델에서는 양수량 차이 및 관정 스크린 혹은 관정의 심도 등의 관정 제원을 고려한 Well Contribution Index (WCI) 라는 지수를 도입하여 최적의 양수-처리 전략을 제안하고자 하였다. 상대적인 수행능력을 평가 결과, NSGA-II 는 지하수 정화 관련 상반되는 목적함수들에 대한 다목적 최적화 문제를 풀 때의 수행 능력이 기존 가중치를 추가한 GA보다 괜찮은 것을 검증할 수 있었다. 충적 대수층 모델에서는 우기 때만 집중적으로 양수하였을 때에 효과적인 양수-처리 설계를 할 수 있는 것을 확인하였다. 마지막으로, WCI를 계산했을 때 KDPW-7 관정이 양수-처리에 가장 많이 기여하는 관정임을 확인할 수 있었다. 이전 연구에서 수행한 KDPW-7 관정에서의 양수-처리 시험에서 효과적인 오염정화가 수행한 결과를 제시하였고, 본 연구에서 도입한 WCI가 실제 양수-처리 시나리오에서 우선 선택해야 하는 양수정을 제안할 수

있을 것으로 기대한다.

주요어: 지하수 모델링, 양수-처리, Non-dominated Sorting Genetic Algorithm (NSGA-II), 트리클로로에틸렌 (TCE), 관정별 기여도 지수 (WCI)